

Microgrid Stability Definitions, Analysis, and Examples

IEEE PES Task Force on Microgrid Stability Definitions, Analysis, and Modeling

Mostafa Farrokhbadi¹, Member, IEEE, Claudio A. Cañizares², Fellow, IEEE, John W. Simpson-Porco³, Member, IEEE, Ehsan Nasr⁴, Member, IEEE, Lingling Fan⁵, Senior Member, IEEE, Patricio A. Mendoza-Araya⁶, Member, IEEE, Reinaldo Tonkoski⁷, Member, IEEE, Ujjwol Tamrakar⁸, Student Member, IEEE, Nikos Hatziaargyriou⁹, Fellow, IEEE, Dimitris Lagos¹⁰, Student Member, IEEE, Richard W. Wies¹¹, Senior Member, IEEE, Mario Paolone¹², Senior Member, IEEE, Marco Liserre¹³, Fellow, IEEE, Lasantha Meegahapola, Member, IEEE, Mahmoud Kabalan¹⁴, Member, IEEE, Amir H. Hajimiragha, Senior Member, IEEE, Dario Peralta¹⁵, Marcelo A. Elizondo, Senior Member, IEEE, Kevin P. Schneider¹⁶, Senior Member, IEEE, Francis K. Tuffner¹⁷, Member, IEEE, and Jim Reilly, Senior Member, IEEE

Manuscript received May 1, 2018; revised November 17, 2018 and February 22, 2019; accepted April 6, 2019. Date of publication June 28, 2019; date of current version January 7, 2020. Paper no. TPWRS-00659-2018. (Corresponding author: Claudio A. Cañizares.)

M. Farrokhbadi, C. A. Cañizares, J. W. Simpson-Porco, and D. Peralta are with the Department of Electrical and Computer Engineering, University of Waterloo, Waterloo ON N2L 3G1, Canada (e-mail: m5farrok@uwaterloo.ca; ccanizares@uwaterloo.ca; jwsimpson@uwaterloo.ca; d2peralta@uwaterloo.ca).

E. Nasr is with Microsoft, Redmond, WA 98052 USA (e-mail: ehsan.nasr@microsoft.com).

L. Fan is with the Electrical Engineering Department, University of South Florida, Tampa, FL 33620 USA (e-mail: linglingfan@usf.edu).

P. A. Mendoza-Araya is with the Department of Electrical Engineering, University of Chile, Santiago 8330111, Chile (e-mail: pmendoza@ing.uchile.cl, rodpalma@cec.uchile.cl).

R. Tonkoski and U. Tamrakar are with the Electrical Engineering and Computer Science Department, South Dakota State University, Brookings, SD 57007 USA (e-mail: reinaldo.tonkoski@sdstate.edu; ujjwol.tamrakar@sdstate.edu).

N. Hatziaargyriou and D. Lagos are with the Department of Electrical and Computer Engineering, National Technical University of Athens, Athens 10563, Greece (e-mail: dimitrioslagos@mail.ntua.gr; nh@power.ece.ntua.gr).

R. W. Wies is with the Electrical and Computer Engineering Department, University of Alaska Fairbanks, Fairbanks, AK 99775 USA (e-mail: rwwiesjr@alaska.edu).

M. Paolone is with the Electrical Engineering Department, Ecole Polytechnique fédérale de Lausanne, Lausanne CH-1015, Switzerland (e-mail: mario.paolone@epfl.ch).

M. Liserre is with the Institute of Electrical Engineering and Information Technology, Kiel University, Kiel 24118, Germany (e-mail: ml@tf.uni-kiel.de).

L. Meegahapola is with the Electrical and Biomedical Engineering Department, RMIT University, Melbourne Vic 3000, Australia (e-mail: lasantha@ieee.org).

M. Kabalan is with the School of Engineering, University of St. Thomas, St. Paul, MN 55105 USA (e-mail: mahmoud.kabalan@stthomas.edu).

A. H. Hajimiragha is with the Energy Research Institute at Nanyang Technological University (ERI@N), Singapore, 637553 (e-mail: amir.miragha@ntu.edu.sg).

M. A. Elizondo, K. P. Schneider, and F. K. Tuffner are with the Pacific Northwest National Laboratory, Richland, WA 99354 USA (e-mail: marcelo.elizondo@pnnl.gov; kevin.schneider@pnnl.gov; francis.tuffner@pnnl.gov).

J. Reilly is with the Reilly Associates, Pittston, PA 18640 USA (e-mail: j_reilly@verizon.net).

Color versions of one or more of the figures in this paper are available online at <http://ieeexplore.ieee.org>.

Digital Object Identifier 10.1109/TPWRS.2019.2925703

Abstract—This document is a summary of a report prepared by the IEEE PES Task Force (TF) on Microgrid Stability Definitions, Analysis, and Modeling, IEEE Power and Energy Society, Piscataway, NJ, USA, Tech. Rep. PES-TR66, Apr. 2018, which defines concepts and identifies relevant issues related to stability in microgrids. In this paper, definitions and classification of microgrid stability are presented and discussed, considering pertinent microgrid features such as voltage-frequency dependence, unbalancing, low inertia, and generation intermittency. A few examples are also presented, highlighting some of the stability classes defined in this paper. Further examples, along with discussions on microgrid components modeling and stability analysis tools can be found in the TF report.

Index Terms—Classification, definitions, microgrids, stability.

I. INTRODUCTION

A MICROGRID is defined as a group of Distributed Energy Resources (DERs), including Renewable Energy Sources (RES) and Energy Storage Systems (ESS), plus loads that operate locally as a single controllable entity [2], [3]. Microgrids can be found in both low and medium voltage operating ranges, typically from 400 V to 69 kV [4]. In addition, they exist in various sizes. They can be large and complex networks, up to tens of MW in size, with various generation resources and storage units serving multiple loads [5]. On the other hand, microgrids can also be small and simple systems, in the range of hundreds of kW, supplying just a few customers [5].

Microgrids have multiple possible configurations depending on their size and functionalities. Thus, they exist in both grid-connected and isolated forms. Hence, grid-connected microgrids have a Point of Interconnection (POI) or Point of Common Coupling (PCC) with a large power network, and should be capable of seamless transition to islanded mode [6]. Note that the islanding capability of microgrids, combined with their ability to black start, increases the resiliency of distribution systems in times of emergency or blackouts [7]. Isolated microgrids have no POI/PCC, thus islanding is not an issue in these systems [8].

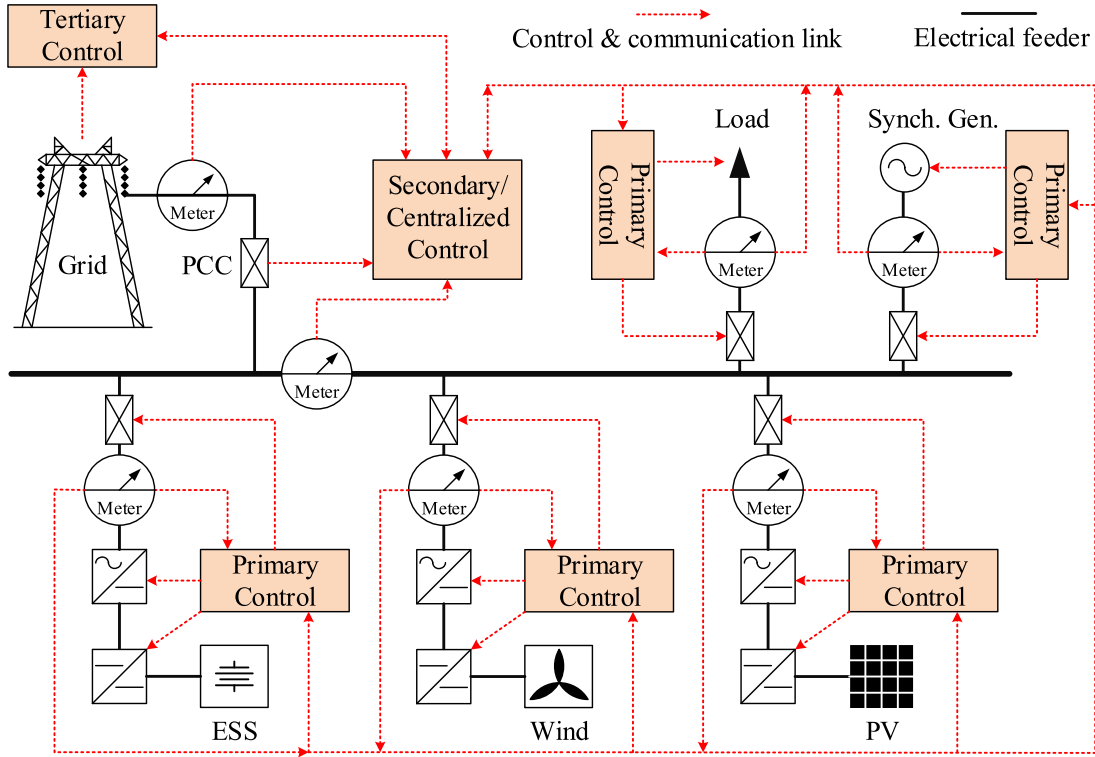


Fig. 1. Typical configuration of a microgrid.

A generic microgrid configuration is shown in Fig. 1, where the system is connected to the main grid via the PCC breaker, and consists of common components such as load, various dispatchable and non-dispatchable DERs, and ESS. As seen in this figure, a microgrid typically contains a communication infrastructure between the Microgrid Central Controller (MGCC), switches, components' primary control, and metering devices. Depending on the upper grid requirements and topology, there may also exist a communication pipeline between the MGCC and a tertiary control layer.

Microgrid control system refers to the set of software and hardware that ensure microgrid operational stability, optimality, and reliability [9], where it is mentioned that the term “microgrid control system” should be adopted over the term “microgrid controller”, implying that the required control functions may be distributed among multiple components rather than being centralized in one controller. Core functions of microgrid control system includes: (i) maintaining the voltages, currents, and frequency within desired ranges; (ii) keeping the power supply and demand balanced; (iii) performing economic dispatch and demand side management; and (iv) transitioning between various modes of operation [3], [9]. As seen in Fig. 1, the microgrid control system can be categorized into three hierarchies, namely, primary, secondary, and tertiary [3].

Microgrid stability is dominantly defined by the primary control, as defined and discussed throughout this paper. This control hierarchy pertains to the fastest control actions in a microgrid, including islanding detection, voltage and frequency control, and power sharing and balance. Several architectures have been proposed for microgrid primary control, including both

centralized and de-centralized approaches [10]. These architectures depend on the microgrid type and purpose, including factors such as grid connectivity, type of grid-forming assets, and required reliability levels. The main variables used for primary control in a microgrid include voltage, frequency, and active and reactive power flows [3]. In grid-connected mode of operation, voltage and frequency are mainly imposed by the main grid, limiting the microgrid role to performing ancillary services. Therefore, the problem of stability in grid-connected microgrids mainly consists of the stability of individual components such as a particular DER or of a set of local loads, including electrical motors, and their impact on the system, as discussed in detail in [11]. With IEEE Standard 1547 allowing for the islanded operation of distribution networks [12], isolated microgrids are expected to play a significant role in smart active distribution grids; in this case, the system voltage and frequency are no longer supported by the main grid, and different DERs must maintain these variables in acceptable ranges. Due to the microgrid unique intrinsic features and systemic differences, discussed in Section II, operation in standalone mode is more challenging than in conventional power systems, facing particular stability and system adequacy problems [13].

Primary control in microgrids with grid-forming synchronous machines is considerably different than inverter-based systems, making stability studies and issues different for each operating paradigm. For example, synchronous machines perform voltage and frequency control and power sharing using conventional exciters, governors, and the machine mechanical inertia. On the other hand, inverter-based DERs rely on a set of fast voltage and current control loops along with Phase-Locked Loops (PLLs),

and thus there is no mechanical time-constant involved in the control process; thus, inverters can be designed to emulate the inertia of a synchronous machine via appropriate controls [14].

This paper considers for the aforementioned aspects of primary control in microgrids, and focuses on stability definitions and classifications for most common microgrid architectures and configurations, including grid-connected, islanded, and inverter-based systems. First, intrinsic differences between microgrids and bulk power systems are highlighted, identifying relevant issues related to stability in microgrids. Definitions and classification of microgrid stability are then presented and discussed, considering pertinent microgrid features and issues pertaining to both electric machines, like induction motors stall, and converters, like PLL-induced instabilities. A few examples are also presented, highlighting some of the stability classes defined in the paper. It is important to highlight the fact that microgrid control and stability mitigation techniques are not in the scope of this paper.

The remaining sections of this document are organized as follows: Section II provides a brief discussion on the microgrid unique characteristics from the system stability perspective. Section III introduces various stability concepts pertinent to microgrids, and proposes proper microgrid stability definitions and classification. Section IV discusses various stability analysis tools and techniques for microgrids. Section V presents and discusses a few relevant examples pertaining to important stability issues in microgrids. Finally, Section VI provides a brief summary and highlights some important conclusions.

II. MICROGRIDS CHARACTERISTICS

The nature of the stability problem and dynamic performance of a microgrid are considerably different than those of a conventional power system, since the microgrid system size is considerably smaller than that of a conventional large interconnected power system. Furthermore, microgrid feeders are relatively short and operated at medium voltage levels, presenting a lower reactance to resistance ratio compared to conventional systems [15]. As a result, the dynamic performance of microgrids and the intrinsic mathematical relationships between voltages, angles, and active and reactive power flows are different than in conventional grids. Another consequence of the microgrid small size is higher uncertainty in the system, due to the reduced number of loads and highly correlated and fast variations of available RES [3].

Demand-supply balance is critical in microgrids, and hence the intermittent nature of RES is particularly relevant in these systems [16]. Bi-directional power flows between generators and prosumers are also an issue [17], due to associated complications with control and protection coordination [3]. In addition, since electric power is supplied by electronically-interfaced DERs and relatively small synchronous machines, system inertia is considerably lower in microgrids compared to conventional power systems. A significant concern in islanded microgrids, especially in remote communities with small distribution systems, is their relatively low short circuit capacity. In such systems, a small change in the microgrid configuration (e.g., start up or shut down

of a diesel genset) can result in relatively large voltage and frequency deviations. This poses stability challenges when operating conventional synchronous generators and inverter-interfaced power generation resources together, since perturbations in this case may lead to inverter shut down [8].

Unlike conventional power systems, loading in microgrids is typically unbalanced [18], which can be as significant as 100% between the three phases [19], [20]. Operating microgrids under such significant unbalanced conditions may jeopardize system stability [21], and requires techniques that are designed to handle these conditions, such as the use of 4-leg voltage source converters (VSCs) proposed in [22]. In addition, traditional stability analysis techniques and models assume balanced operation, and therefore are not valid in unbalanced systems.

Summarizing, the most important differences of microgrids compared to bulk power systems relevant to stability are the following: smaller system size, higher penetration of RES, higher uncertainty, lower system inertia, higher R/X ratio of the feeders, limited short-circuit capacity, and unbalanced three-phase loading. These intrinsic differences between microgrids and bulk power systems require a review of the stability definitions and classification for microgrids with respect to transmission grids, which is the main focus of this paper.

III. DEFINITION AND CLASSIFICATION OF STABILITY IN MICROGRIDS

A. Definitions

Consider a microgrid which is operating in equilibrium, with state variables taking on appropriate steady-state values satisfying operational constraints, such as acceptable ranges of currents, voltages, and frequency [23]. Such a microgrid is stable if, after being subjected to a disturbance, all state variables recover to (possibly new) steady-state values which satisfy operational constraints (e.g., [23]), and without the occurrence of involuntary load shedding. Note that a microgrid that performs voluntary load shedding, under the paradigm of demand response with loads voluntarily participating in the microgrid control [24], is considered stable if it meets the aforementioned conditions. In addition, if loads are disconnected to isolate faulted elements after a disturbance, and not for the sole purpose of shedding load to address voltage and frequency problems, and the microgrid meets the aforementioned conditions, the system can also be considered stable.

In traditional power systems, due to the high number of loads and the large scale of the system, intentional tripping of loads is acceptable to preserve the continuity of its operation [25]; no single load has priority over the stability of the system as a whole. In contrast, microgrids are designed to serve a relatively small number of loads, and hence the operator can prioritize the connectivity of certain feeders (e.g., one that supplies a hospital) over the rest of the system; if such a critical feeder(s) is tripped, the microgrid is no longer achieving its primary objective. Thus, intentional tripping of loads to maintain the operation of the rest of the system during or after a disturbance, other than the specific ones previously mentioned, renders the system unstable by the definition presented in this paper.

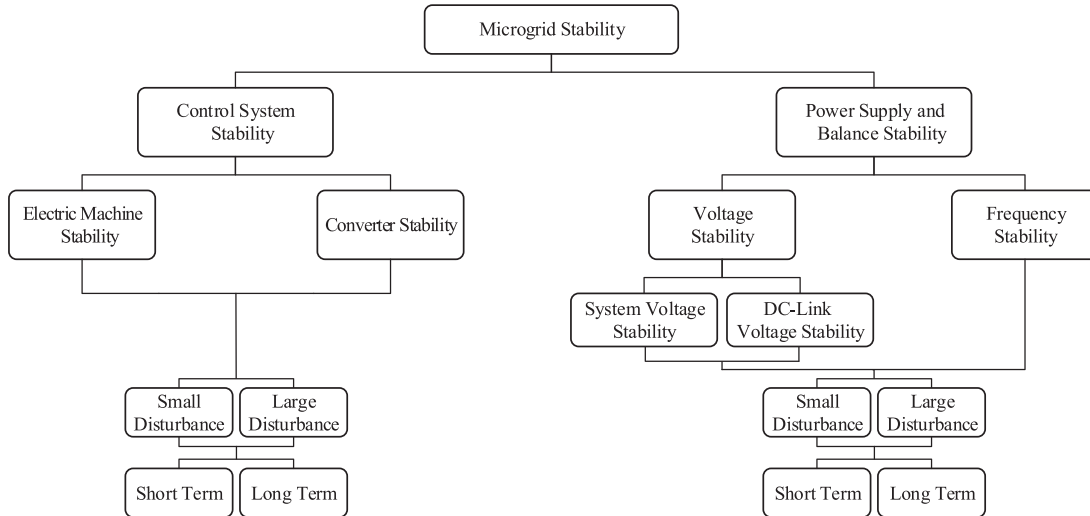


Fig. 2. Classification of stability in microgrids.

In the above definition, disturbances correspond to any exogenous inputs, and may be associated with load changes, component failures, or operational mode/set-point adjustments. If the disturbances are considered to be “small”, so that a linearized set of equations can adequately represent the system behavior, these are classified as small-perturbations, as usual. Otherwise, the disturbances are referred to as large disturbances, which include short-circuits, unplanned transitions from grid-connected to islanded mode of operation, and loss of generation units. It is important to note that planned islanding results in much less significant voltage and frequency excursions, since the DERs set-points are calculated and adjusted accordingly prior to islanding.

Depending on the root cause, small-perturbation instability can be either a short-term or a long-term phenomenon. For example, poor power sharing among multiple DERs can yield undamped power oscillations growing quickly beyond acceptable operating ranges in the short term. On the other hand, heavily loaded microgrids may show undamped oscillations with small load changes in the long term.

B. Classification

Due to the unique characteristics of microgrids mentioned in Section I, new types of stability issues can be observed in these systems. For example, in conventional systems, transient and voltage stability problems typically occur more often than frequency stability ones, whereas in isolated/islanded microgrids, maintaining frequency stability is more challenging due to the low system inertia and a high penetration of RES. In addition, some stability problems observed in large interconnected systems, such as inter-area oscillations and voltage collapse, have not been observed in microgrids. Thus, there is a need to review and modify the power system stability classifications in [26] to properly reflect relevant stability issues in microgrids.

Stability in microgrids can be categorized according to the physical cause of the instability, the relative size of the

disturbance, the physical components that are involved in the process, the time-span during which the instability occurs, and the methodology to analyze or predict the instability, as in [26]. Voltage and frequency are strongly coupled in microgrids, and thus, contrary to some instability phenomena in conventional systems, instability in microgrids is manifested by fluctuations in all system variables. This strong coupling between system variables makes it quite difficult to classify instability phenomena as “voltage instability” or “frequency instability” based solely on measurements of the respective variables. Given this difficulty, the more useful classification scheme proposed here places more emphasis on the type of the equipment and/or controllers that are involved in the instability process triggered by a system disturbance.

Based on the aforementioned discussion, Fig. 2 illustrates the classification of stability in microgrids proposed here. Hence, stability in microgrids should be divided into two main categories: phenomena pertaining to the equipment control systems, and phenomena pertaining to active and reactive power sharing and balance. Note that microgrid instability in either category can be a short- or long-term phenomena; short-term stability issues have a time frame of up to a few seconds, while other issues beyond this time frame pertain to long term stability of the system. The rest of this section discusses the stability types depicted in Fig. 2.

C. Power Supply and Balance Stability

Power Supply and Balance Stability pertains to the ability of the system to maintain power balance, and effectively share the demand power among DERs, so that the system satisfies operational requirements. These types of stability issues are associated with the loss of a generation unit, violation of DERs limits, poor power sharing among multiple DERs, wrong selection of slack(s) resources [27], and/or involuntary no-fault load tripping. In addition, certain type of loads, such as constant power loads or induction motors, may trigger certain types of

instability in the system, such as voltage and harmonic problems. This class of stability can be subcategorized into Frequency and Voltage Stability, as discussed next.

1) *Frequency Stability*: Frequency regulation is a major concern in isolated/islanded microgrids, due to the systemic features explained in Section I, including low system inertia and a high share of intermittent RES. In addition, the low number of generation units in microgrids puts the system at risk of large disturbances in the event of generator outages. Therefore, for such disturbances, the system frequency may experience large excursions at a high rate of change, jeopardizing the system frequency stability [28], [29]. In this context, conventional frequency control techniques and technologies may not be fast enough to overcome the rapid change of system frequency, even in the presence of sufficient generation reserve [30]. Actual examples of such events have been reported around the world [31].

Strong coupling between voltage and frequency in microgrids further complicates frequency regulation. First, due to the high R/X ratios of microgrid feeders, the conventional decoupling of active power flow and voltage magnitudes is no longer valid [32]. Second, because of the relatively small scale of microgrids, voltage changes at the DERs terminals are almost instantaneously reflected on the load side, which in turn changes the system demand depending on the load voltage sensitivity indices [33]–[35]. Therefore, this voltage-frequency coupling should be accounted for in the stability analysis and control of frequency in microgrids.

Frequency instability can be triggered for a variety of reasons in microgrids. For example, a large load increase accompanied by inadequate system response can result in a fast decay of frequency, due to low system inertia, leading to a system blackout triggered by the protection scheme [28]. Poor coordination of multiple frequency controllers and power sharing among DERs may trigger small-perturbation stability issues resulting in undamped frequency oscillations in the span of a few seconds to a few minutes [36], a phenomenon rarely observed in large grids. Hence, depending on the time it takes for the frequency protection schemes to trip the system, this may result in a long-term frequency instability. Insufficient generation reserve can also lead to the steady-state frequency being outside acceptable operating ranges, activating under-frequency load tripping relays, as in large grids. On the other hand, traditional long-term frequency instabilities in larger grids pertaining to steam turbine overspeed controls and boiler and reactive protection and control schemes (e.g., [26]) are not relevant in microgrids.

2) *Voltage Stability*: In conventional power systems, a major root cause of voltage instability is long transmission lines, which limit the power transfer between generation and loads. However, in microgrids, the feeders are relatively short, resulting in relatively small voltage drops between the sending and receiving ends of the feeders [18], [33]. Thus, voltage collapse, i.e., the slow and sustained decay of voltage associated with load recovery process and reactive power supply capacity, has not been observed in microgrids. Nevertheless, with the current distribution networks evolving into microgrids, voltage drops

and current limits may become an issue, in particular for weaker and older grids [37].

In microgrids, the limits of DERs and the sensitivity of load power consumption to supplied voltage are critical factors in voltage instability. Thus, in these systems, voltage instabilities in the form of unacceptable low steady-state and dynamic voltages may occur. Furthermore, in microgrids with high penetration of induction motors, fault induced delayed voltage recovery (FIDVR), as defined for transmission systems [38], can be an issue; thus, since faults in microgrids may drop the system voltage to as low as 0.2 pu [6], induction motors may absorb up to three times their nominal reactive power to re-magnetize, a phenomenon referred to as motor stall, leading to system voltage instability or large load shedding due to insufficient supply of reactive power [39], [40]. This is a particularly challenging issue to address, due to difficulties with managing reactive power sharing among DERs in a microgrid, as explained next.

In bulk power systems, reactive power is mostly managed locally by regulating the voltage at the terminals of generators and compensated loads. However, in microgrids, the feeders are short, and thus any changes in the DER terminal voltages are almost immediately reflected in the rest of the system [41]. Thus, system voltage controls are mostly associated with DERs, rather than FACTS, OLTCs, or switched capacitors, which are not commonly found in microgrids. These controls directly affect the voltage of all system buses, and hence proper coordination of DER QV droops are necessary. In fact, small differences in voltage magnitudes at DERs, if not properly coordinated, may yield high circulating reactive power flows and thus result in large voltage oscillations [42].

Proper reactive power sharing among multiple DERs in a microgrid is most commonly done in practice through voltage-reactive power droop, similar to multiple generator plants in large power systems. As in the case of classical active power-frequency droop, under the voltage-reactive power droop paradigm, the output voltage-magnitude reference of a DER linearly decreases as its reactive power injection increases [10]; thus, DERs with steeper voltage-reactive power droop slopes have a higher contribution to the reactive power supply of the system. This droop mechanism typically does not achieve the desired reactive power sharing, for three main reasons [43]. First, unlike frequency, voltage magnitude varies, albeit slightly, throughout the system, and thus local voltage measurements cannot be easily used to enforce global reactive power sharing. Second, the concept of voltage droop has been developed based on the premise that the lines are inductive, thus reactive power flow is tightly coupled with voltage magnitude; however, as discussed in Section I, such an assumption is generally not valid in microgrids. Finally, the relation between the system voltage and reactive power consumption is determined by the load voltage sensitivity, which is nonlinear in general. To address these drawbacks, other communication-based techniques for effective reactive power load sharing among parallel DERs in microgrids have been proposed, such as isochronous power load sharing [30]; however, special care is needed in this case when communicating the reactive power load sharing data.

Another type of voltage instability in microgrids pertains to the ability of VSC-based DERs to maintain the voltage across the dc-link capacitor. Depending on the DER type, this voltage is maintained via a buck/boost converter or a dc/ac inverter; either way, the voltage ripples across the capacitor depend on the injected/absorbed instantaneous power. Therefore, it may occur that when active power injections of the inverter are close to their limits, an increase in reactive power demand may result in undamped ripples in the voltage across the dc-link capacitor; as a result, large fluctuations appear in the active and reactive power injection of DERs [21].

Depending on the system response and load characteristics, a voltage instability may occur following a large disturbance, such as a sudden change in the demand and/or output of RES, or a generator outage. Small disturbances, such as small incremental changes in the demand can also result in voltage instabilities, in particular for systems which are close to their loading limits or are highly unbalanced [21].

In terms of the time-frame, voltage instability can be a short- or a long-term phenomenon. Short-term voltage instabilities arise from poor control coordination, or fast dynamics changes in the active and/or reactive power mismatch. On the other hand, long-term voltage instabilities pertain to DERs output limits being gradually reached by a steady increase in the demand, as in the case of thermoelectrical loads.

D. Control System Stability

Control System Stability issues may arise due to inadequate control schemes (e.g., harmonic resonance of parallel DERs) and/or poor tuning of one or more pieces of equipment controllers. In the latter case, the poorly tuned controller(s) is the primary source of instability, and the system cannot be stabilized, as per the definitions provided in Section II-A, until the controller is re-tuned or the associated piece of equipment is disconnected. This type of stability pertains to electric machines and inverters control loops, LCL filters, and PLLs. This category of stability is subcategorized into Electric Machine and Converter Stability, as explained next.

1) *Electric Machine Stability*: Conventionally, these types of stability studies are concerned with the ability of synchronous machines to return to synchronism with the rest of the system following the angular acceleration of these machines during a fault. However, this phenomenon has not been observed in microgrids. For example, due to the resistive nature of microgrids, synchronous machines may decelerate during short circuits if fault occurs at the end of the feeder; this is demonstrated in the experimental results discussed in [44].

In conventional power systems, small-perturbation stability issues can be manifested either by an aperiodic increase or undamped oscillations of the rotor angle of the synchronous generators [45]. The former instability occurs due to the lack of synchronizing torque, while the latter happens because of inadequate damping torque. However, in the context of microgrids, synchronizing and damping torque problems have not been observed in generators equipped with well-tuned voltage regulators and governors. From the aforementioned discussions,

electric machine stability in microgrids is dominantly associated with poor tuning of synchronous machines' exciters and governors [20].

2) *Converter Stability*: In microgrids, inverters are prone to small- and large-perturbation instabilities. Inner voltage and current control loops are a major concern for small-perturbation stability of the system, since their tuning is a challenging issue in practice. In addition, a system blackout after large disturbances due to tripping of DERs, in particular inverter-based RES due to under-frequency and under-voltage protection schemes, are a serious concern.

Contrary to low-frequency oscillations caused by outer power controls, interaction of inner current and voltage control loops may cause high harmonic-frequency oscillations, in the range of hundreds of Hz to several kHz [46], [47], a phenomenon referred to as harmonic instability. In this context, harmonic instability is an "umbrella term" used in the technical literature for a range of phenomena resulting in high harmonic-frequency oscillations, including resonance and multi-resonance issues. The presence of several inverters at close proximity also generates interaction problems resulting in multi-resonance peaks [48]. Another root-cause of harmonic instability is high-frequency switching, triggering parallel and series resonances introduced by LCL power filters or parasitic feeder capacitors [46], [49]. The resonance of an inverter LCL filter can be also triggered by the control of the inverter itself or by interactions with controllers nearby [50]. Harmonic instability can be prevented and/or mitigated by so called active damping strategies [47], [51].

The wide usage of grid synchronization strategies based on PLLs in grid-following/feeding inverters modifies the admittance matrices of the power system, which may lead to instabilities [52]. It has been shown that a PLL introduces a negative parallel admittance to the input admittance, which jeopardizes the stability of the system [53]. This effect can affect the system voltages, and can be mitigated by reducing the PLL bandwidth [54]; however, low-bandwidth PLLs may cause stability issues, in particular in heavily-loaded microgrids, as shown in Section III-A. Furthermore, low voltages can affect the PLL-based synchronization strategies in VSCs, since in this case, the PLL may fail to properly detect zero crossings of network voltages [55].

E. Large vs. Small Disturbance

In the context of microgrids, large disturbances include short-circuits, unplanned transitions from grid-connected to islanded mode of operation, and loss of generation units. Large disturbances can result in large frequency and voltage excursions and power swings among multiple DERs [56]. Such problems can be due to various reasons, such as a critical system mode being pushed to the unstable region by the fault, causing undamped oscillations in the system; similar behavior is observed during the unintentional islanding of a grid-connected microgrid [6]. Hence, proper power coordination among DERs and the response time of their controllers is critically important for retaining the stability of the system [6], [56]. In terms of the time-frame, stability issues due to large disturbances in microgrids can be classified as short-term phenomena, i.e., in the order of a few seconds.

TABLE I
CHARACTERISTICS OF VARIOUS TYPES OF STABILITY ISSUES IN MICROGRIDS

Category	Control System Stability		Power Supply and Balance Stability	
Subcategory	Electric Machine Stability	Converter Stability	Voltage Stability	Frequency Stability
Root Cause	Poor controller tuning.	Poor controller tuning, PLL bandwidth, PLL synchronization failure, harmonic instability.	DERs power limits, inadequate reactive power supply, poor reactive power sharing, load voltage sensitivities, dc-link capacitor.	DERs active power limits, inadequate active power supply, poor active power sharing.
Manifestation	Undamped oscillations, aperiodic voltage and/or frequency increase/decrease.	Undamped oscillations, low steady-state voltages, high-frequency oscillations.	Low steady-state voltages, large power swings, high dc-link voltage ripples.	High rate of change of frequency, low steady-state frequency, large power and frequency swings.

It is important to note that planned islanding results in much less significant voltage and frequency excursions, since the DERs set-points are calculated and adjusted accordingly prior to islanding. When this transition takes place, one of the DERs in the island should be running in frequency-regulating/load-following/grid-forming mode. The time delay involved in this event, which may take a few cycles, adds to the complexity of maintaining microgrid stability. This is particularly an issue when the islanding is unplanned, microgrid has no or little inertia, and the exchanged power with the utility prior to disconnection is large (e.g., 50% of the local microgrid demand). In this case, over- or under-voltages may appear within a few cycles that could trip the inverters safety, resulting in the islanded microgrid becoming rapidly unstable.

As in bulk power systems, in microgrids, a disturbance is considered small if a linearized set of equations can adequately represent the system behavior [26], [45]. In this context, small-perturbation stability dominantly pertains to sustained oscillations arising from low-damped critical eigenvalues following a small disturbance. Depending on the root cause, small-perturbation instability can be either a short-term or a long-term phenomenon. For example, poor coordination of power sharing schemes among multiple DERs can yield undamped power oscillations growing quickly beyond acceptable operating ranges in the short term. On the other hand, heavily loaded microgrids in the long term, may show undamped oscillations with small load changes.

F. Summary

In microgrids, due to system characteristics such as feeder length and R/X ratios, a strong coupling exists between system variables such as active and reactive power flows, as well as voltage and frequency; such couplings are more evident under stressed conditions associated with instability issues. Hence, it is important to properly identify the major root causes of the instability problem; Table I summarizes these based on the aforementioned discussions and describes the way that each type of instability may manifest itself in the system.

IV. ANALYSIS TECHNIQUES AND TOOLS

Stability studies start with the definition of the initial system conditions, typically computed using power flow techniques. These techniques allow to perform static studies such as the determination of voltage profiles in microgrids [20], [57].

A. Large-Perturbation Stability

Microgrids show highly non-linear dynamics [58], but typically microgrid stability studies have been based on small-perturbation linearization techniques [59]. Various bodies of work are demonstrating that small-perturbation stability might not give as an accurate representation of stability in microgrids [60], [61]. The presence of power electronic converters and stochastic resources which can exhibit large dynamic changes makes the large-perturbation stability critical for microgrids. When faults occur in an isolated/islanded microgrid, or a fault triggers an unintentional islanding of a microgrid, Critical Clearing Times (CCTs) can give a good idea of the relative stability. In [45], the CCT is defined as the maximum time between initiation and isolation of a fault such that the power system remains stable. Classical equal area criterion analysis is helpful in determining CCTs in transmission systems; however, in microgrids, this technique does not apply, as stability problems are not directly associated with synchronism problems among DERs, as discussed in Section II. Large-perturbation stability analysis in microgrids can be performed using two main approaches: Lyapunov-based stability studies [61], [62], time-domain simulations carried out on accurate models of a microgrid [6], [20], and Hardware-in-the-Loop (HIL) approaches [63].

1) *Lyapunov Techniques*: Several Lyapunov approaches have been reported in the literature [59], [64]–[66]. An advantage of Lyapunov’s direct method is that the non-linear differential equations associated with the system do not need to be solved analytically for transient stability analysis [67]. Large-perturbation stability of various microgrid components have been discussed in the literature using Lyapunov based techniques [68], [69], such as for synchronous generators, inverters, rectifiers, and dc/dc converters. For example, in [69], an electrostatic machine based model for inverters are derived, which allows for easier small- and large-perturbation stability analysis of these systems. Lyapunov techniques can then be used on the derived “equations of motion” to analyze the large-perturbation stability. Compared to small-perturbation studies, Lyapunov techniques have the following advantages: (1) the domain of validity and effectiveness of Lyapunov techniques is larger than that of small-perturbation analysis methods, (2) the proper representation of nonlinear power electronic converters, and (3) the adequate capture of large transient events experienced by renewable energy sources such as solar PV and wind. A system that is stable (as defined by Lyapunov-based techniques) is small-perturbation stable,

but the reverse is not always true. Thus, Lyapunov techniques give better insights on the transient stability of microgrids. Successfully applying Lyapunov techniques to microgrids presents several challenges. First, finding the proper Lyapunov function is a significant hurdle and requires many simplifying assumptions; hence, these techniques have been limited to balanced three-phase systems. Moreover, studies that explore the dynamic interactions of power electronic converters and electromechanical systems have yet to be carried out using Lyapunov-based techniques. Additionally, Lyapunov functions can be nontrivial, so there is a need for systematic mathematical approaches that could be adopted widely with different generator and load models. Furthermore, modeling the microgrids as non-autonomous or time-varying systems is a challenging and nontrivial issue that adds another level of complexity.

2) *Time-Domain Simulations*: Large-perturbation stability analysis of microgrid systems using time-domain simulations, based on accurate models of the system components and loads, of the type found in EMT tools [70], is the most effective way to investigate stability issues in microgrids, as reported in the literature [20], [71]. Time-domain simulations have some advantages over Lyapunov-based techniques, including higher accuracy and validity. On the other hand, time-domain simulations of non-linear systems are computationally intensive and typically many such simulations are required to ensure system stability over a wide variety of initial conditions and disturbances. It is also noteworthy that stability boundaries derived using time-domain simulations are precise, albeit expensive to obtain, and thus result in proper resource utilization of microgrids, as opposed to Lyapunov techniques.

Ideally, EMT tools should be used for time-domain simulations in microgrids, since they model all components in detail; however, for larger microgrids, this might be infeasible due to the computational complexities and burden. Electromechanical transient tools, also known as Transient Stability (TS) tools has been developed and used to address these computational issues in system transient studies, but these tools have been traditionally designed for balanced networks, and thus are not suitable for unbalanced microgrid studies. An intermediate solution could be provided by capturing unbalances in TS simulations, using phasor dynamic models that capture network and stator dynamics around the fundamental frequencies [72]–[74]. TS simulations are proposed for microgrids/distribution systems with unbalanced modeling in [75], with dynamic phasors in [76], and with transitions between dynamics and power flows solutions in [77].

3) *Hardware-in-the-Loop Studies*: Real-time HIL simulations have proven to be an advanced and efficient tool for the analysis and validation of microgrids, in particular DER components and their controls. The two main classes of real time HIL testing are Controller Hardware in the Loop (CHIL) and Power Hardware in the Loop (PHIL), as depicted in Fig. 3 and discussed next.

In CHIL simulations, a hardware controller is tested and connected to a microgrid network simulated entirely in a Digital Real Time Simulator (DRTS). For example, CHIL can be used to test an inverter controller, where the controller sends the

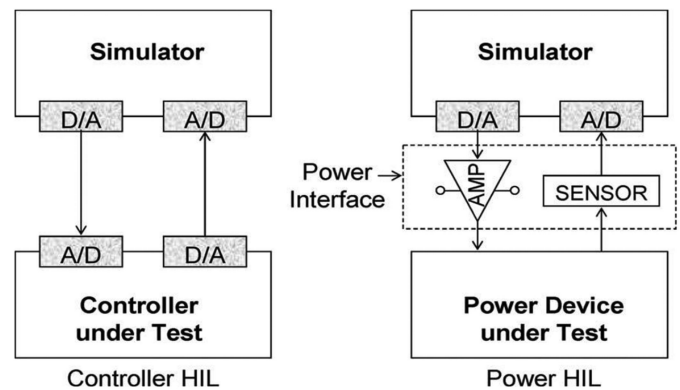


Fig. 3. PHIL and CHIL setup [63].

PWM signals to the DRTS, which feeds back voltage and current measurements as analogue signals. A power system controller (e.g. distribution management system, microgrid control system) can also be tested with CHIL, where the signal exchange between the controller and the DRTS can be performed by digital or analog signals or via communication protocols. The advantages of CHIL testing compared to time-domain simulations are significant. Thus, DRTSs are able to solve the microgrid's mathematical equations in real time, allowing the implementation of control algorithms on a physical hardware controller, interfaced with the DRTS in real time. In addition, CHIL simulations can reveal weaknesses in the control algorithms, studying their performance under various realistic conditions such as time delays and noise, and interacting with complex power system models, thus providing valuable insights in control system stability issues [78].

In a PHIL setup, a part of the microgrid is simulated in great detail in a DRTS integrated with real hardware. In order to connect the hardware to a node of the simulated microgrid, an amplifier is used as an interface between the DRTS and the equipment. The amplifier receives as input a reference signal from the DRTS and provides the respective voltage value to the equipment, and a current sensor is utilized to transfer the current from the hardware to the simulator. This setup allows the user to test real equipment hardware under various circumstances, and to study the impact of the hardware on the system [79].

B. Small-Perturbation Stability

Conventionally, small-perturbation stability of a power system is studied through eigenvalue analysis by developing state-space models of the system. Efforts have been made to develop accurate state-space models of various microgrid components, such as inverters, the network, and dynamic loads [36], [80]. These studies reveal that critical low-frequency modes are highly affected by the tuning of inverters outer power sharing control loops, whereas the critical high-frequency modes are dominated by the inverter inner voltage and current control loops. However, such state-space approaches are rather complex to develop for unbalanced networks, while microgrids in general are unbalanced systems, which is an important factor in determining the overall system stability in microgrids [20].

In this context, a combination of dynamic simulations and signal-processing methods such as the Prony technique have been shown to be effective studying the small-perturbation stability [20], [33]. Another drawback in classical state-space based approaches is that the validity and magnitude of the linearization domain is unknown. Small perturbations can be explored without an explicit knowledge of what constituents “small”. In traditional power systems with large inertia and with an infinite bus, such disturbances are not likely to substantially perturb the system from its current operating state. However, since microgrids have a smaller inertia and no infinite bus, small perturbations are more likely to significantly affect the system. This document presents a classification of stability in microgrids based primarily on the equipment origin of the potential instability (e.g., inner control loop tunings, PLL bandwidth issues, etc.). This approach is taken to avoid classical frequency/voltage categorizations, as these variables are strongly coupled by microgrid dynamics. However, if faced with an instability, one must ultimately identify the true source of the problem. Small-perturbation stability analysis via linearization provides a useful tool for identifying the origin of the instability, by studying the left and right eigenvectors of the dynamic system matrix. For example, in the case of a Control System Stability problem, it is likely to have state variables with large components in the right eigenvectors of the linearized system pertaining to a particular piece of equipment. On the other hand, in the case of a Power Supply and Balance Stability issue, it is expected to have a wider range of state variables, corresponding to various equipments, to have larger components in the linearized system eigenvectors.

V. EXAMPLES

A few relevant examples of microgrid instabilities are presented and discussed here. More examples can be found in [1], along with discussion on various models.

A. Voltage-Frequency Dependency

To demonstrate some of the aforementioned stability phenomena and issues in isolated/islanded microgrids, the CIGRE benchmark for medium voltage distribution network introduced in [18], has been implemented in PSCAD/EMTDC. This microgrid has a 1.3 MVA diesel-based synchronous machine, a 1 MW ESS, and a 1 MW wind turbine, with the latter being modeled using an average model presented in [21]. The diesel-based synchronous machine and its exciter and governor are tuned and validated according to actual measurements for the diesel gensets discussed in [19]. The loads are modeled using the static exponential model with a 1.5 exponent, which is a reasonable value for typical isolated microgrids [35].

In this case, the diesel generator is connected and is the master voltage and frequency controller, and the ESS is providing 0.5 MW of active power in the grid-feeding mode. The wind turbine is generating 300 kW of active power, and the load scaled so that the total system demand is 1.6 MW and 0.2 MVar, balanced among the three phases. At $t = 1$ s, the wind generator active power output is decreased to 50 kW. In addition, to demonstrate the impact of voltage changes on the

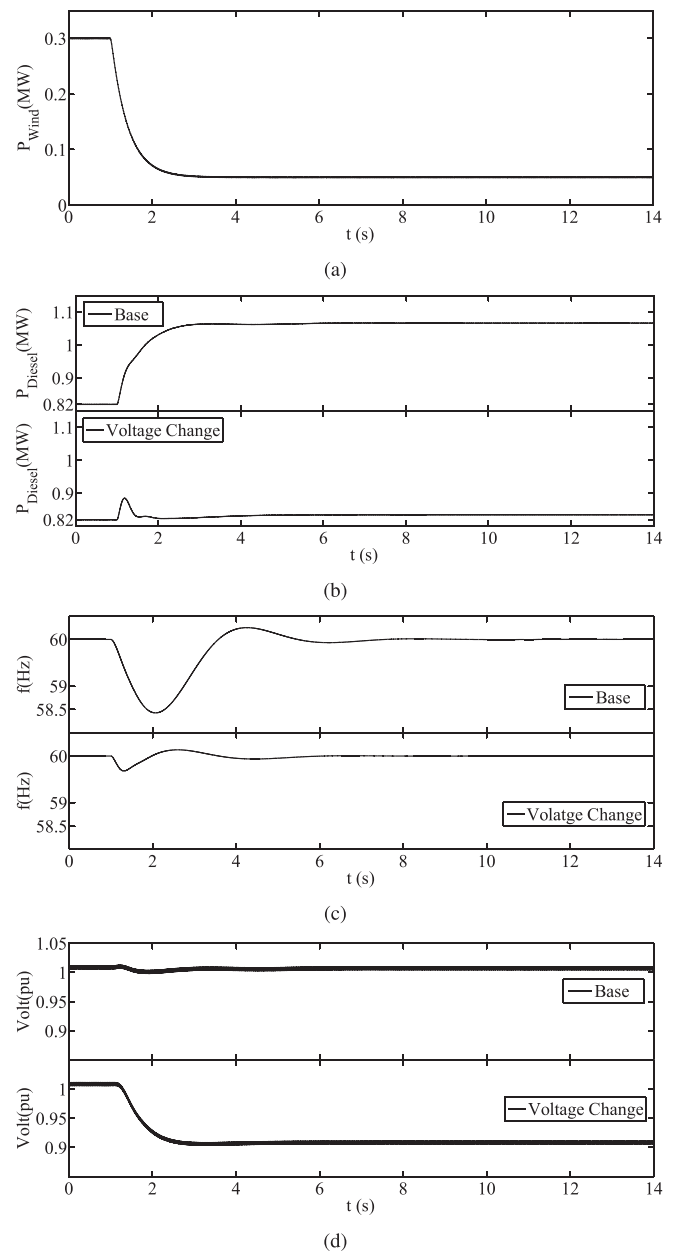


Fig. 4. Voltage-frequency dependency: (a) wind turbine active power, (b) diesel engine active power, (c) frequency, and (d) RMS voltage at PCC bus.

system frequency, a -0.1 step change is passed through a lag filter with a time constant of 0.4 s, and is then added to the machine voltage regulator set-point, to simulate the effect of the Voltage-Frequency Controller (VFC) [33].

Figure 4 shows the wind power output, diesel engine active power, system frequency, and the RMS voltage at the PCC bus. Note in these figures that the voltage change has a considerable impact on the system frequency response, compensating for the power mismatch in the system due to the wind power reduction. As seen in Fig. 4(b), the diesel engine active power output barely increases when the system voltage changes, compared to a 250 kW increase for the base system. This is due to the linkage between the voltage magnitude and active power

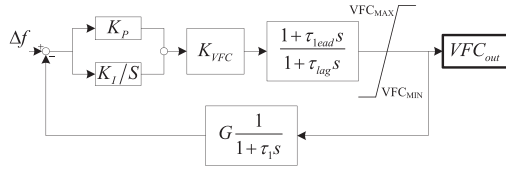


Fig. 5. Modified version of the VFC in [33].

TABLE II
VFC PARAMETERS

VFC Parameters				
K_P	K_I	K_{VFC}	τ_{lead}	τ_{lag}
0.04	0.154	1	0.04	0.001
VFC_{Max}	VFC_{Min}	G	τ_1	
0.1	-0.1	2.5	0.1	

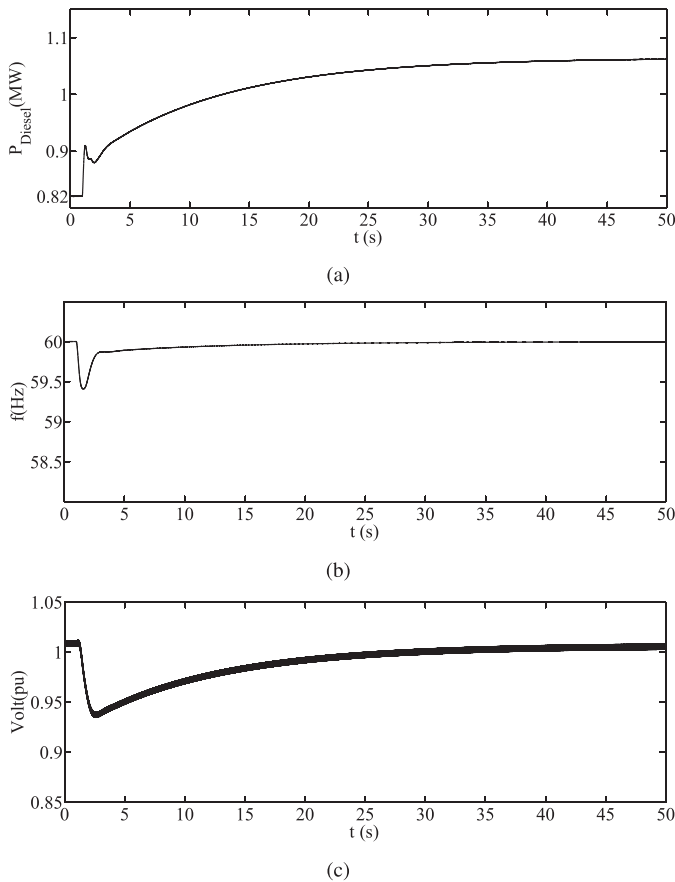


Fig. 6. Case C with VFC: (a) diesel engine active power; (b) frequency, and (c) RMS voltage at PCC.

consumption [35], which is the base of the VFC proposed in [33]. Thus, a closed-loop version of the (VFC) is demonstrated here, as shown in Fig. 5.

The parameters of the VFC in Fig. 5 are shown in Table II, and are first estimated based on the Ziegler-Nichols tuning technique, and then refined experimentally. Fig. 6 shows the frequency response of the system with the modified VFC is much improved compared to the base system. In addition, the voltage steady-state error is zero, due to the negative feedback loop of the VFC. This is an example of Frequency Stability in microgrids,

discussing a control mitigation approach based on the particular characteristics of microgrids.

B. Impact of the PLL Synchronization Loop Bandwidth

A three-bus system, shown in Fig. 7, is implemented in a real-time digital simulator. The typical current control scheme for the grid-connected inverter at Bus 2 is used, as in [21]. An equivalent ZIP model of the inverter using such current control as well as a PLL can be represented by:

$$\begin{aligned}
 \begin{bmatrix} \Delta i_d \\ \Delta i_q \end{bmatrix} &= \overbrace{\begin{bmatrix} Y_{dd} & 0 \\ 0 & Y_{qq} \end{bmatrix} \begin{bmatrix} \Delta v_d \\ \Delta v_q \end{bmatrix}}^{\text{Z-component}} + \overbrace{\begin{bmatrix} I_{dd} & 0 \\ 0 & I_{qq} \end{bmatrix} \begin{bmatrix} \Delta i_{dref} \\ \Delta i_{qref} \end{bmatrix}}^{\text{I-component}} \\
 &+ \begin{bmatrix} \theta_{d1} \\ \theta_{q1} \end{bmatrix} \Delta \theta' \\
 &= \begin{bmatrix} Y_{dd} & 0 \\ 0 & Y_{qq} \end{bmatrix} \begin{bmatrix} \Delta v_d \\ \Delta v_q \end{bmatrix} + \begin{bmatrix} I_{dd} & 0 \\ 0 & I_{qq} \end{bmatrix} \begin{bmatrix} \Delta i_{dref} \\ \Delta i_{qref} \end{bmatrix} \\
 &+ \begin{bmatrix} 0 & \theta_{d1} G_{PLL_op(s)} \\ 0 & \theta_{q1} G_{PLL_op(s)} \end{bmatrix} \begin{bmatrix} \Delta v_d \\ \Delta v_q \end{bmatrix} \quad (1)
 \end{aligned}$$

where i_{dref} , i_{qref} , i_d , i_q , v_d , and v_q are the current references, grid currents, and grid voltages in the dq frame, respectively; and Y_{dd} , Y_{qq} , I_{dd} , and I_{qq} are the equivalent admittance and current components of the inverter when the PLL is not considered, with the corresponding constant power component being zero. The effects of synchronization, represented by the PLL open-loop transfer function G_{PLL_op} , can be considered as part of the constant impedance component.

As shown in Fig. 8, when the load at Bus 3 increases at $t = 3.5$ s and maximum loadability is approached, a converter with a slow PLL will result in a system collapse, as shown in Fig. 8(a), while a fast PLL can keep the system stable, as illustrated in Fig. 8(b). This is an example of Control System Stability, and particularly Converter Stability.

C. Parallel Converter Droop Control Issues

This example demonstrates that oscillations can occur in parallel converters with V-I droop control [81], when the droop control parameters for the two converters are set differently. These types of oscillations are not observed if the parallel converters are modeled as an aggregated converter or their droop parameters are the same, reflecting a Power Supply and Balance Stability issue.

Figure 9 depicts the test system. The V-I droops are implemented as described in [36], and m_k and n_k are active and reactive power droops respectively. As seen in Fig. 10, if both of m_k and n_k are small, the system becomes unstable, unless the droop coefficients are larger and/or $m_1 = m_2$ and $n_1 = n_2$, which make the system stable. These poorly damped modes are caused by circulating currents which are basically dq -axis currents going back and forth between the DER units. These

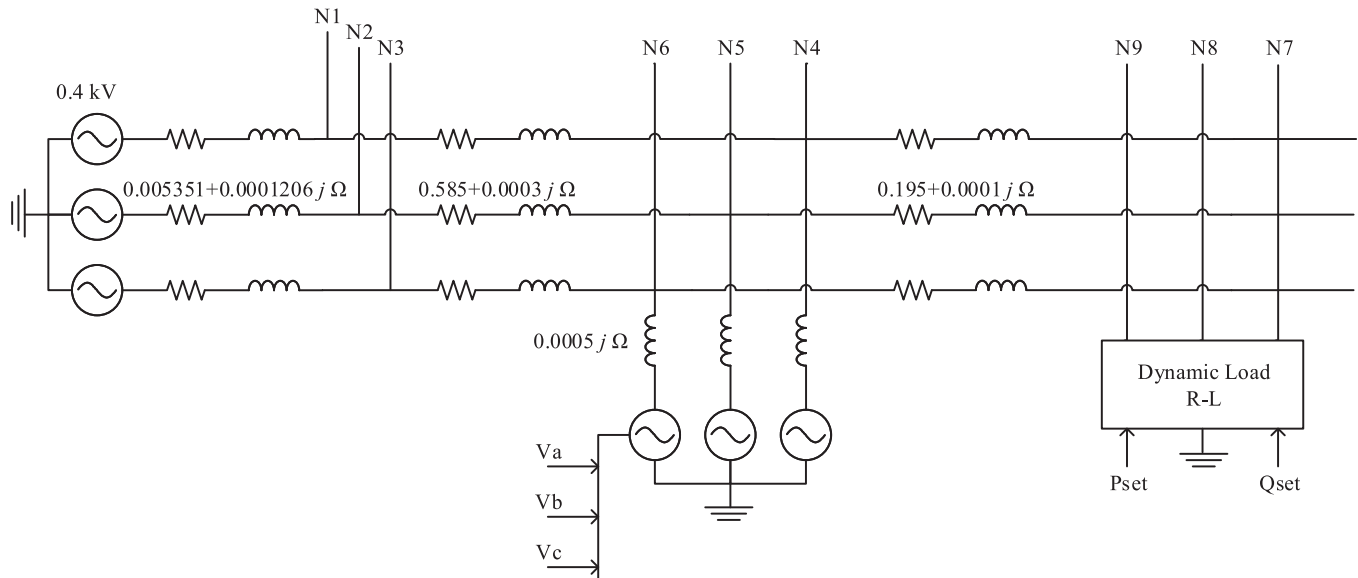


Fig. 7. Three-bus test system for PLL stability studies.

results can be verified with time-domain simulations; more results can be found in [1]. This is an example of Power Supply and Balance Stability, since the problem is not one poorly tuned DER, but the coordination of multiple DERs.

D. Impact of Load Dynamics

In order to compare the characteristics of different load types (e.g., static loads, Direc-on-Line (DOL) loads, Variable Speed-Drive (VSD) loads), a three-phase short-circuit fault was simulated on the microgrid shown in Fig. 11, which comprises a total load of 60 kW, with each load type having equal capacity, i.e., 20 kW for each static, DOL, and VSD loads. The static load is represented by a ZIP load model with a 0.85 lagging power factor, and has equal proportion of constant current, power, and impedance load. The DOL motor load is represented by a fan load, and the VSD motor load is represented by a pump load; more details can be found in [1]. Initially, the microgrid is operated in grid-connected mode, but does not exchange active power with the main grid. The solar PV system generates 35 kW, the diesel generator generates 20 kW, and the battery energy storage system injects 5.5 kW to maintain the power balance in the microgrid.

Figure 12 represents the active and reactive power for each load type, following a 150 ms three-phase short-circuit fault, with a fault impedance of $0.1 + j0.1$ pu at the microgrid 400 V busbar during grid-connected and islanded modes. Observe that the different load types result in substantially different system responses during the short-circuit fault. Both the static and DOL motor loads' active and reactive power consumption substantially decrease during the fault, and recover rapidly following fault clearance. However, unlike the static load, the DOL motor load requires substantial reactive power during the recovery phase, i.e., three times the rated reactive power, even though limited by a soft-starter; this would affect the overall stability of the microgrid. The VSD motor load is less affected in grid-connected mode, and maintains almost the same active and reactive power consumption. However, in islanded mode,

the VSD motor load trips due to commutation failure at the front-end rectifier [82], resulting in active and reactive power decreasing to zero, as shown in Fig. 12(c).

Figure 13 illustrates the various loads' dynamic responses following a 12 kW load switching event, (20% load increase) in the microgrid for grid-connected and islanded modes. All three load types have negligibly affected during the load switching event when operating in grid-connected mode; however, in islanded mode, 0.05% – 5% oscillations are observed in all three load types. This example shows the importance of the load characteristics for microgrid stability.

E. Virtual Inertia Mitigation Techniques

Virtual (Synthetic) inertia has been widely proposed in the literature as a solution for low inertia issues. Some of the most popular topologies involve a synchronverter [14], virtual synchronous machines (VISMA) [83], Ise Lab's topology [84], synchronous power controllers (SPC) [85], VSYNC topology [86], virtual oscillator control [87], and others. Droop controllers used in parallel operation of DERs have also been shown to provide virtual inertia under certain conditions [88]. The basic concept is the same in all of these techniques, with the aim of replicating inertial response through control algorithms and power electronic converters [89]. The required energy can be obtained through ESS or curtailed operation of DERs. One of the basic requirements of these systems is that they operate autonomously and quickly (from a few cycles to less than 10 s) to counter-act the fast decay of frequency in low-inertia microgrid systems. Fig. 14 shows a typical configuration of a virtual-inertia system, with the virtual-inertia algorithm at the core of the system. The controller senses the frequency of the system typically using a PLL. Based on the frequency measurements and its rate-of-change, power references can be generated for the inverter as follows:

$$P_{VI} = K_D \Delta\omega + K_I \frac{d\Delta\omega}{dt} \quad (2)$$

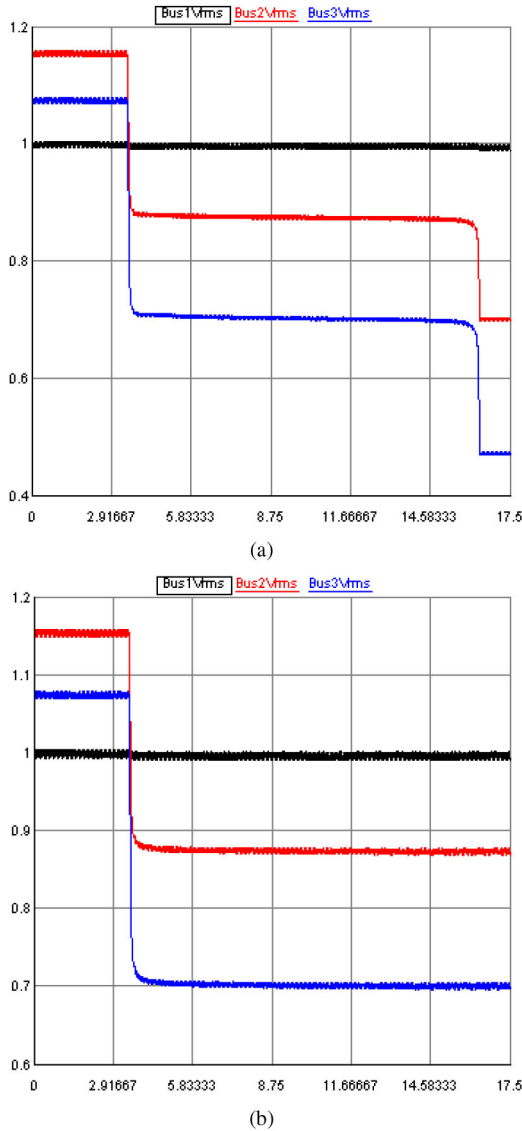


Fig. 8. PLL test system voltages in pu: (a) 5.7 Hz PLL, and (b) 20 Hz PLL.

where $\Delta\omega$ and $d\Delta\omega/dt$ are the change in frequency and its rate of change (ROCOF), respectively. K_D and K_I are the damping and the inertia constants, respectively.

More sophisticated control approaches like the synchronverter, VSIMA, SPC, etc., try to mimic the exact dynamics of a synchronous generator either through detailed equations or some kind of approximation. Virtual-inertia algorithms are already implemented in commercial inverters; however, certain challenges still remain in the integration of virtual-inertia systems in the context of microgrids. Improved control design, aggregation of multiple virtual inertia units and energy usage minimization are a few of the challenges that need to be addressed [90].

1) *Benchmark PV-Hydro Microgrid System*: To demonstrate the impact of high renewable penetration in the frequency stability of microgrids, a PV-hydro benchmark system, introduced in [89], is used here. This benchmark system consists of a 39 kVA hydro generator and a 25 kWp PV system, as shown in Fig. 15.

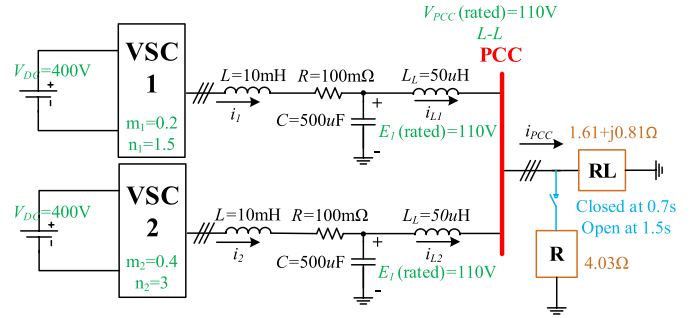


Fig. 9. Droop control test system [81].

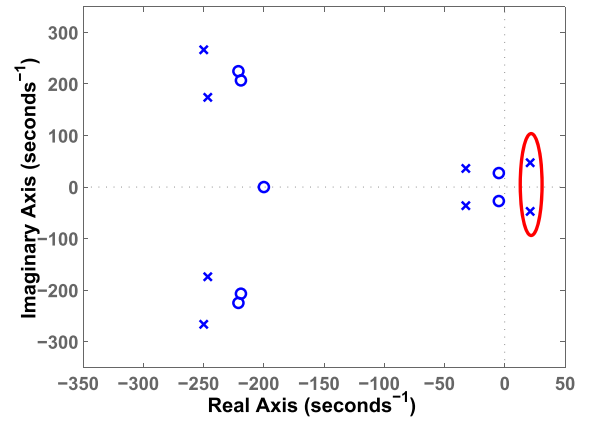


Fig. 10. Location of dominant poles in droop control for $m_1 = 0.004$, $m_2 = 0.008$, $n_1 = 0.01$, and $n_2 = 0.02$.

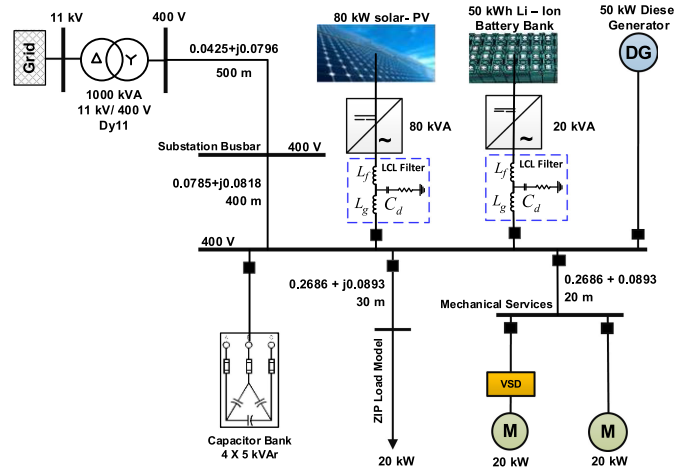


Fig. 11. Microgrid test system for dynamic load studies.

The hydro unit was adapted from the remote village of Bhujung in Nepal, scaling it to match the PV installation at the South Dakota State University (SDSU) Microgrid Research laboratory. The microgrid is a three-phase system operating at 208 V with a rated frequency of 60 Hz. The PV is modeled using current sources with no inertial response, whose magnitude depends on the available solar irradiance. High penetration of intermittent PV in such systems can lead to frequency stability, as fast

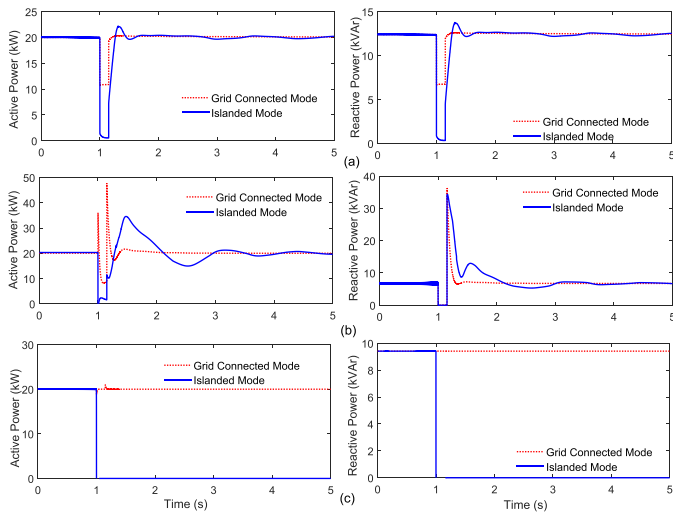


Fig. 12. Dynamic characteristics of different load types during a fault in a microgrid: (a) static (ZIP) load, (b) DOL motor load, and (c) VSD motor load.

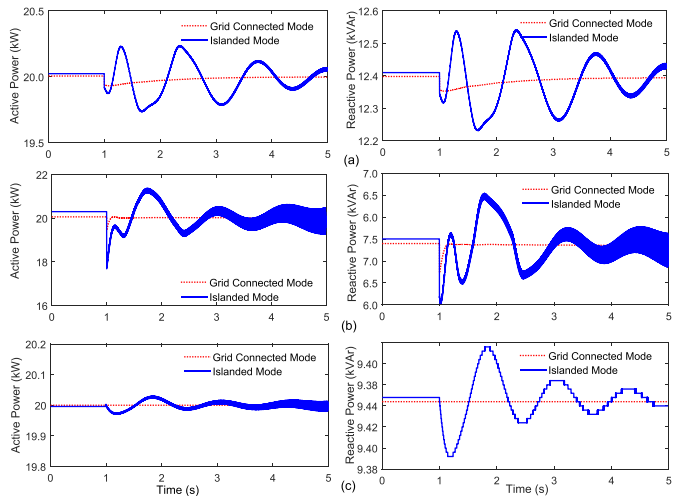


Fig. 13. Dynamic response of different load types during a 20% load switch event in the.

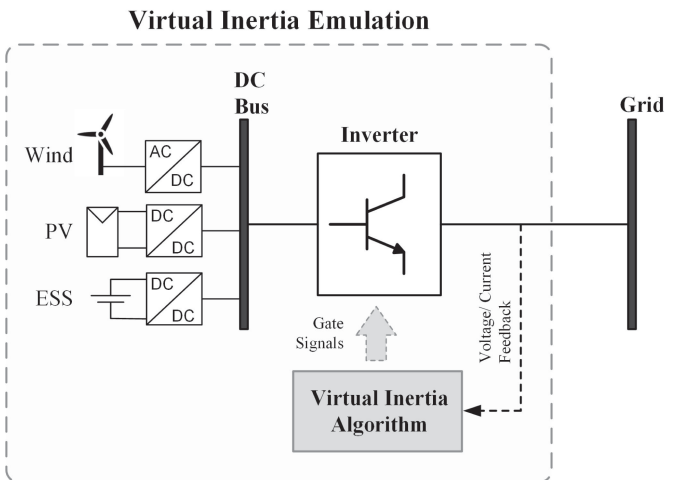


Fig. 14. Virtual-inertia using a power electronic converter.

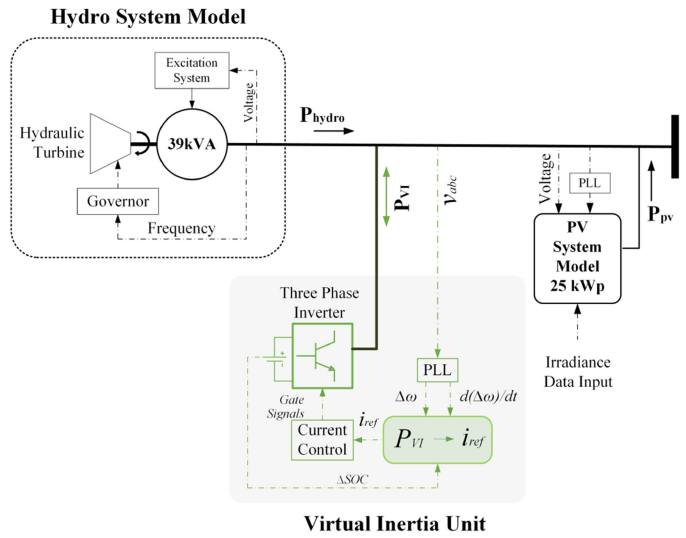


Fig. 15. Virtual-inertia unit implemented in a benchmark PV-hydro microgrid system.

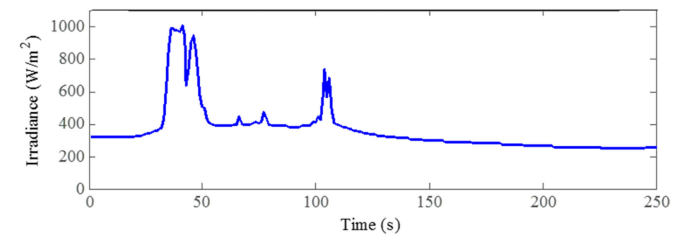


Fig. 16. Snapshot of irradiance data for July 19, 2012 (sampling rate is 1 s).

changes in PV generation cannot be absorbed by the relative low inertia of the small-hydro system.

The test system was analyzed using a 250 s snapshot of real irradiance data, as shown in Fig. 16. The frequency variations were obtained for three different levels of PV penetration, i.e., 10, 15, and 25 kWp, as shown in Fig. 17. Large frequency variations outside the ISO8528 recommended limits for generators [91] can be observed; with increased PV penetration, the magnitude of the frequency excursions are much higher. The ROCOF are extremely high (as high as 4.8 Hz/s for 25 kWp penetration). This affects the frequency stability of the system, since such conditions can trigger frequency relays leading to cascading failures of generation units in a microgrid.

Simulations are then performed with a dedicated inverter emulating virtual inertia installed in the system, as shown in Fig. 15. The frequency of the system for 25 kWp PV penetration after addition of virtual inertia is shown in Fig. 18 with solid lines. The reduction in the ROCOF and the frequency excursions are summarized in Table III. The maximum and minimum frequency excursions can be reduced by 6.3% and 4.7%, respectively; similarly, the maximum ROCOF can be reduced by as much as 85.4%. After the addition of VI, both the frequency and its rate of change are within the permissible limits.

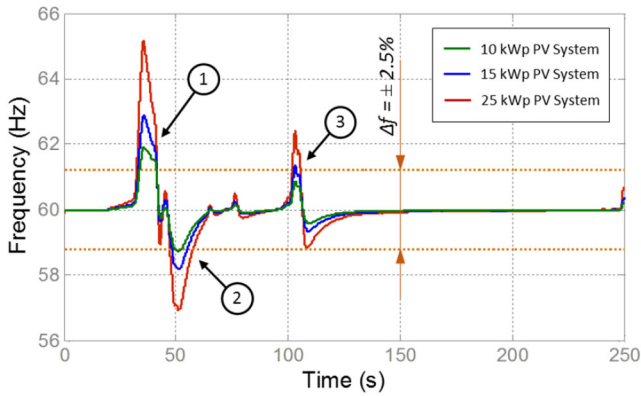


Fig. 17. Frequency variations observed in the PV-hydro benchmark system for PV penetration levels of 10, 15, and 25 kWp.

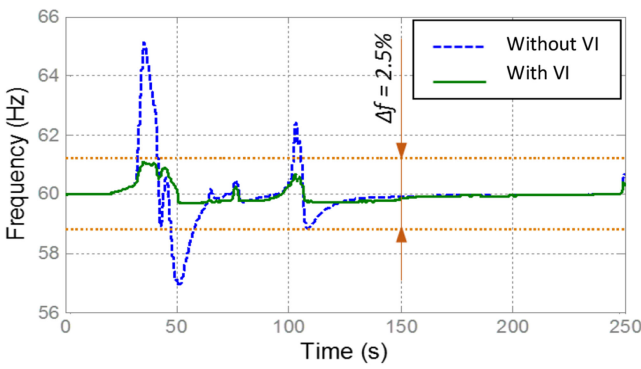


Fig. 18. Reduction in frequency deviations in the PV-hydro benchmark with virtual inertia unit.

TABLE III
COMPARISON OF FREQUENCY VARIATION AND ROCOF WITH AND WITHOUT VIRTUAL INERTIA

	Without Virtual Inertia	With Virtual Inertia
Minimum Frequency	56.9 Hz	59.6 Hz
Maximum Frequency	65.1 Hz	61.0 Hz
Maximum ROCOF	4.8 Hz/s	0.7 Hz/s

F. Isolation and Reconnection of a Microgrid

One of the desired features of a microgrid is its capability of disconnection from and re-synchronization to a larger grid, in cases such as faults and intentional islanding. In this example [92], a small perturbation stability analysis of pre- and post-isolation shows how the system could become unstable.

The microgrid under study is shown in Fig. 19, where two inverter-interfaced DERs, each rated at 10 kW, feed local loads, with the possibility of grid connection through a static switch. The microgrid model includes realistic distribution line parameters, as well as coupling transformers for each DER.

The system eigenvalues for the islanded case are stable for a droop gain of DER 1 between 5% to 20%, while maintaining the droop gain of DER 2 at 5%; the results of sweeping the droop gain of DER 2 are similar. The system eigenvalues for the grid-tied case for the same droop gains show that the system becomes unstable for values above 16%, which is a relatively

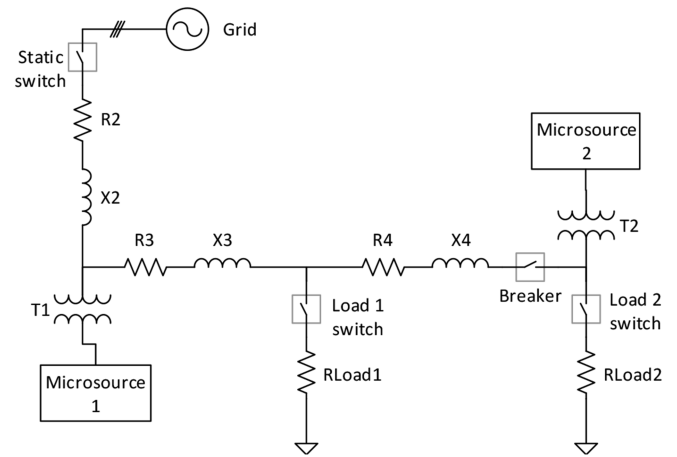


Fig. 19. Simulation model of a microgrid for islanding and synchronization analysis.

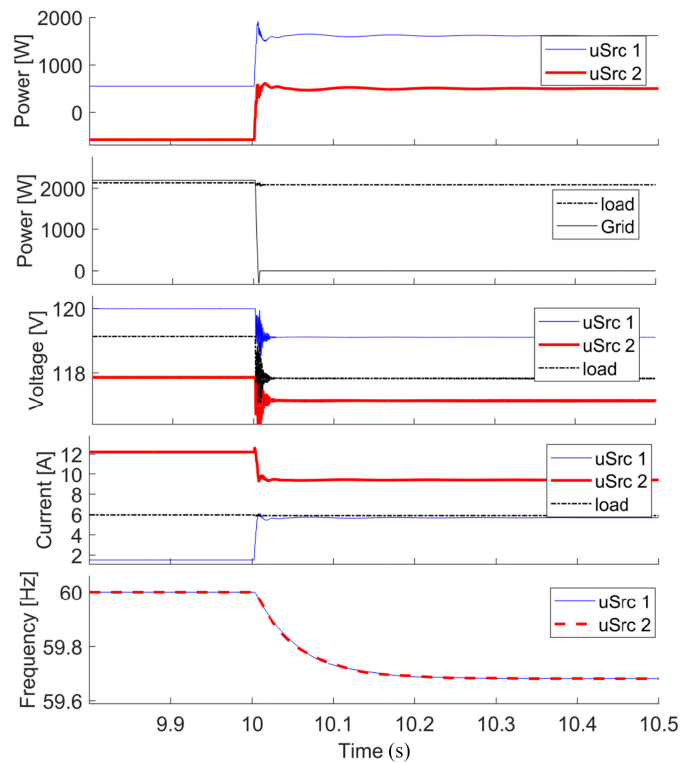


Fig. 20. Simulation results for microgrid islanding: stable case.

high droop gain in the sweeping range used for testing purposes. These results are verified by time-domain simulations. Thus, Fig. 20 illustrates the case of microgrid islanding, when the droop gains of DERs 1 and 2 are at 5%. Observe that, when the static switch is opened at $t = 10$ s, the microgrid transits into an island seamlessly, with a reduction in frequency due to the droop control, and the power of the impedance load decreasing due to the voltage drop. It is worth noting that, before islanding, both DERs feed power proportional to their set-points, with the grid feeding the load and part of the microgrid losses. After the transition, both sources feed the load according to

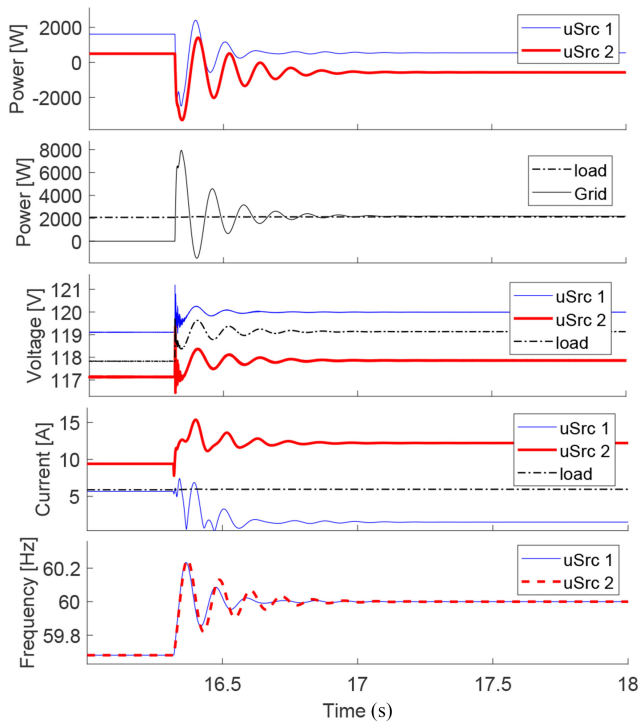


Fig. 21. Simulation results for microgrid synchronization: stable case.

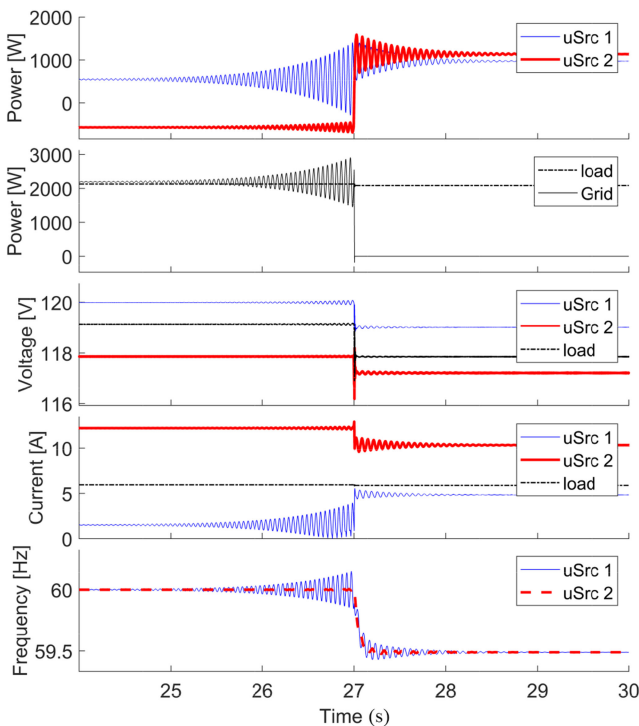


Fig. 22. Simulation results for microgrid disconnection: unstable case.

their power and frequency set-points, with a frequency drop of 0.3 Hz.

Figure 21 shows the microgrid re-synchronization process starting at $t = 16.3$ s. Observe that the microgrid presents poor damping, but otherwise the synchronization is stable. The droop

gains of the DERs are again at 5%, thus ensuring stability. This particular result set is an example of Power Supply and Balance Stability issue, since both inverters are similarly tuned, and oscillations arise from poor power sharing between the DERs rather than a poorly tuned inverter.

Figure 22 illustrates the case of the microgrid in grid-tied mode, with the droop gain of DER 1 being increased from 5% to 20% at $t = 20$ s. As expected from the eigenvalues studies, the system is unstable in this case. The time-domain simulation shows that before $t = 27$ s, the power and frequency waveforms of DER 1 and the grid show sustained oscillations until $t = 27$ s, when the static switch is opened and the microgrid is islanded, reaching stable operation after a few seconds. This is an example of Control System Stability, since the droop gain of one individual inverter is unrealistically high, i.e., it is poorly tuned for grid-tied operation.

VI. CONCLUSION

Due to their unique characteristics, microgrids present stability issues different from those observed in bulk power systems; therefore, this document focused on presenting microgrid stability definitions, classifications, and examples. Thus, definitions of microgrid stability issues were presented, classifying instabilities in microgrids based on their fundamental causes and manifestations, and illustrating relevant microgrid stability issues through some examples. Further examples, along with discussions on stability modeling and analysis tools are provided in [1].

ACKNOWLEDGMENT

The authors would like to thank Prof. A. Sumper and Dr. M. Aragues from the Polytechnic University of Catalonia for their valuable input.

REFERENCES

- [1] M. Farrokhhabadi *et al.*, "Microgrid stability, definitions, analysis, and modeling," IEEE Power and Energy Society, Piscataway, NJ, USA, Tech. Rep. PES-TR66, Apr. 2018.
- [2] B. Lasseter, "Microgrids (distributed power generation)," in *Proc. Power Eng. Soc. Winter Meet.*, Jan. 2001, pp. 146–149.
- [3] D. E. Olivares *et al.*, "Trends in microgrid control," *IEEE Trans. Smart Grid*, vol. 5, no. 4, pp. 1905–1919, Jul. 2014.
- [4] N. Hatziaargyriou, H. Asano, R. Iravani, and C. Marnay, "Microgrids," *IEEE Power Energy Mag.*, vol. 5, no. 4, pp. 78–94, Jul. 2007.
- [5] A. Hirsch, Y. Parag, and J. Guerrero, "Microgrids: A review of technologies, key drivers, and outstanding issues," *Renewable Sustain. Energy Rev.*, vol. 90, pp. 402–411, Jul. 2018.
- [6] F. Katiraei, M. Iravani, and P. W. Lehn, "Micro-grid autonomous operation during and subsequent to islanding process," *IEEE Trans. Power Del.*, vol. 20, no. 1, pp. 248–257, Jan. 2005.
- [7] J. M. Guerrero *et al.*, "Distributed generation: Toward a new energy paradigm," *IEEE Ind. Electron. Mag.*, vol. 4, no. 1, pp. 52–64, Mar. 2010.
- [8] A. H. Hajimiragha and M. R. D. Zadeh, "Research and development of a microgrid control and monitoring system for remote community of Bella Coola: Challenges, solutions, achievements, and lessons learned," in *Proc. Int. Conf. Smart Energy Grid. Eng.*, Aug. 2013, pp. 1–6.
- [9] *IEEE Standard For the Specification of Microgrid Controllers*, IEEE Std. 2030.7, 2018.
- [10] J. M. Guerrero, M. Chandorka, T. Lee, and P. C. Loh, "Advanced control architectures for intelligent microgrids—Part I: Decentralized and hierarchical control," *IEEE Trans. Ind. Electron.*, vol. 60, no. 4, pp. 1254–1262, Apr. 2012.

- [11] T. van Cutsem *et al.*, "Contribution to bulk system control and stability by distributed energy resources connected at distribution network," IEEE Power and Energy Society, Piscataway, NJ, USA, Tech. Rep. PES-TR22, Jan. 2017.
- [12] *IEEE Guide For Design, Operation, and Integration of Distributed Resource Island Systems With Electric Power Systems*, IEEE Std. 1547.4, 2011.
- [13] F. Katiraei, R. Iravani, N. Hatziaargyriou, and A. Dimeas, "Microgrids management," *IEEE Power Energy Mag.*, vol. 6, no. 3, pp. 54–65, Jun. 2008.
- [14] Q. C. Zhong and G. Weiss, "Synchronverters: Inverters that mimic synchronous generators," *IEEE Trans. Ind. Electron.*, vol. 58, no. 4, pp. 1259–1267, Apr. 2011.
- [15] C. Li, S. K. Chaudhary, M. Savaghebi, J. C. Vasquez, and J. M. Guerrero, "Power flow analysis for low-voltage ac and dc microgrids considering droop control and virtual impedance," *IEEE Trans. Smart Grid*, vol. 8, no. 6, pp. 2754–2764, Mar. 2016.
- [16] C. Yuen, A. Oudalov, and A. Timbus, "The provision of frequency control reserves from multiple microgrids," *IEEE Trans. Ind. Electron.*, vol. 58, no. 1, pp. 173–183, Jan. 2011.
- [17] A. Ipakchi and F. Albuayeh, "Grid of the future," *IEEE Power Energy Mag.*, vol. 7, no. 2, pp. 52–62, Apr. 2009.
- [18] K. Strunz *et al.*, "Benchmark systems for network integration of renewable and distributed energy resources," CIGRE, Paris, France, Tech. Rep. C6.04.02, Apr. 2014.
- [19] M. Arriaga, "Long-term renewable energy generation planning for off-grid remote communities," Ph.D. Thesis, Univ. Waterloo, Waterloo, ON, Canada, 2015.
- [20] E. Nasr-Azadani, C. A. Cañizares, D. E. Olivares, and K. Bhattacharya, "Stability analysis of unbalanced distribution systems with synchronous machine and DFIG based distributed generators," *IEEE Trans. Smart Grid*, vol. 5, no. 5, pp. 2326–2338, Sep. 2014.
- [21] M. Farrokhabadi, S. Konig, C. Cañizares, K. Bhattacharya, and T. Leibfried, "Battery energy storage system models for microgrid stability analysis and dynamic simulation," *IEEE Trans. Power Syst.*, vol. 33, no. 2, pp. 2301–2312, Aug. 2017.
- [22] C. Burgos-Mellado *et al.*, "Experimental evaluation of a CPT-based four-leg active power compensator for distributed generation," *IEEE J. Emerg. Sel. Topics Power Electron.*, vol. 5, no. 2, pp. 747–759, Jun. 2017.
- [23] "Distributed generation technical interconnection requirements: Interconnections at voltages 50 kV and below," Hydro One Networks Inc., Toronto, ON, Canada, Tech. Rep. DT-10-015 R3, Mar. 2013.
- [24] J. Wang, H. Zhang, and Y. Zhou, "Intelligent under frequency and under voltage load shedding method based on the active participation of smart appliances," *IEEE Trans. Smart Grid*, vol. 8, no. 1, pp. 353–361, Jan. 2017.
- [25] C. W. Taylor, "Concepts of undervoltage load shedding for voltage stability," *IEEE Trans. Power Del.*, vol. 7, no. 2, pp. 480–488, Apr. 1992.
- [26] P. Kundur *et al.*, "Definition and classification of power system stability," *IEEE Trans. Power Syst.*, vol. 19, no. 2, pp. 1387–1401, May 2004.
- [27] A. Bernstein, J. L. Boudec, L. Reyes-Chamorro, and M. Paolone, "Real-time control of microgrids with explicit power setpoints: Unintentional islanding," in *Proc. IEEE PowerTech*, Eindhoven, The Netherlands, Jul. 2015, pp. 1–6.
- [28] G. Dellile, B. Francois, and G. Malarange, "Dynamic frequency control support by energy storage to reduce the impact of wind and solar generation on isolated power system's inertia," *IEEE Trans. Sustain. Energy*, vol. 3, no. 4, pp. 931–939, Oct. 2012.
- [29] A. Borghetti, C. A. Nucci, M. Paolone, G. Ciappi, and A. Solari, "Synchronized phasors monitoring during the islanded maneuver of an active distribution network," *IEEE Trans. Smart Grid*, vol. 2, no. 1, pp. 82–91, Mar. 2011.
- [30] A. H. Hajimiragha, M. R. Dadash Zadeh, and S. Moazeni, "Microgrids frequency control considerations within the framework of the optimal generation scheduling problem," *IEEE Trans. Smart Grid*, vol. 6, no. 2, pp. 534–547, Mar. 2015.
- [31] N. Hatziaargyriou, E. Karapidakis, and D. Hatzifotis, "Frequency stability of power systems in large islands with high wind power penetration," in *Proc. Bulk Power Syst. Dyn. Control Symp.-IV Restructuring*, 1998, vol. PAS-102, pp. 1501–1504.
- [32] K. Christakou, J. Y. LeBoudec, M. Paolone, and D. C. Tomozei, "Efficient computation of sensitivity coefficients of node voltages and line currents in unbalanced radial electrical distribution networks," *IEEE Trans. Smart Grid*, vol. 4, no. 2, pp. 741–750, Jun. 2013.
- [33] M. Farrokhabadi, C. A. Cañizares, and K. Bhattacharya, "Frequency control in isolated/islanded microgrids through voltage regulation," *IEEE Trans. Smart Grid*, vol. 8, no. 3, pp. 1185–1194, Oct. 2015.
- [34] M. Diaz-Aguilo *et al.*, "Field-validated load model for the analysis of CVR in distribution secondary networks: Energy conservation," *IEEE Trans. Power Del.*, vol. 28, no. 4, pp. 2428–2436, Oct. 2013.
- [35] G. Delille, L. Capely, D. Souque, and C. Ferroillat, "Experimental validation of a novel approach to stabilize power system frequency by taking advantage of load voltage sensitivity," in *Proc. IEEE Eindhoven PowerTech*, Eindhoven, The Netherlands, Jun. 2015, pp. 1–6.
- [36] N. Pogaku, M. Prodanovic, and T. C. Green, "Modeling, analysis and testing of autonomous operation of an inverter-based microgrid," *IEEE Trans. Power Electron.*, vol. 22, no. 2, pp. 613–625, Mar. 2007.
- [37] R. Prada and L. Souza, "Voltage stability and thermal limit: Constraints on the maximum loading of electrical energy distribution feeders," *IEEE Proc. Gener. Transmiss. Distrib.*, vol. 145, no. 5, pp. 573–577, Sep. 1998.
- [38] NERC Transmission Issues Subcommittee and System Protection and Control Subcommittee, "A technical reference paper fault-induced delayed voltage recovery," North Amer. Elect. Reliability Corp., Princeton, NJ, USA, Tech. Rep. 1.2, Jun. 2009.
- [39] J. Zhao, D. Shi, R. Sharma, and C. Wang, "Microgrid reactive power management during and subsequent to islanded process," in *Proc. IEEE PES T&D Conf. Expo.*, Chicago, IL, USA, Apr. 2014, pp. 1–5.
- [40] J. Elizondo, P. Huang, J. L. Kirtley, and M. S. Elmoursi, "Enhanced critical clearing time estimation and fault recovery strategy for an inverter-based microgrid with IM load," in *Proc. IEEE PES General Meeting*, Boston, MA, USA, Jul. 2016, pp. 1–5.
- [41] B. Solanki, C. A. Cañizares, and K. Bhattacharya, "Practical energy management systems for isolated microgrids," *IEEE Trans. Smart Grid*, to be published, doi: [10.1109/TSG.2018.2868130](https://doi.org/10.1109/TSG.2018.2868130).
- [42] C. K. Sao and P. W. Lehn, "Autonomous load sharing of voltage source converters," *IEEE Trans. Power Del.*, vol. 20, no. 2, pp. 1009–1016, Aug. 2016.
- [43] W. Yao, M. Chen, J. Matas, J. M. Guerrero, and Z. Qian, "Design and analysis of the droop control method for parallel inverters considering the impact of the complex impedance on the power sharing," *IEEE Trans. Ind. Electron.*, vol. 58, no. 2, pp. 576–588, Feb. 2011.
- [44] R. Belkacemi, S. Zarrabian, A. Babalola, and R. Craven, "Experimental transient stability analysis of microgrid systems: Lessons learned," *IEEE Trans. Power Del.*, vol. 28, no. 4, pp. 2428–2436, Oct. 2013.
- [45] P. Kundur, *Power System Stability and Control*. New York, NY, USA: McGraw-Hill, 1994.
- [46] X. Wang, F. Blaabjerg, and W. Wu, "Modeling and analysis of harmonic stability in an ac power-electronic-based power system," *IEEE Trans. Power Electron.*, vol. 29, no. 12, pp. 6421–6432, Dec. 2014.
- [47] X. Wang, F. Blaabjerg, and Z. Chen, "Autonomous control of inverter-interfaced distributed generation units for harmonic current filtering and resonance damping in an islanded microgrid," *IEEE Trans. Ind. Appl.*, vol. 50, no. 1, pp. 452–461, Jan. 2014.
- [48] J. He, Y. W. Li, D. Bosnjak, and B. Harris, "Investigation and active damping of multiple resonances in a parallel-inverter-based microgrid," *IEEE Trans. Power Electron.*, vol. 28, no. 1, pp. 234–246, Jan. 2013.
- [49] X. Wang, F. Blaabjerg, M. Liserre, Z. Chen, J. He, and Y. Li, "An active damper for stabilizing power-electronic-based ac systems," *IEEE Trans. Power Electron.*, vol. 29, no. 7, pp. 3318–3329, Jul. 2014.
- [50] M. Liserre, F. Blaabjerg, and S. Hansen, "Design and control of an LCL-filter based three-phase active rectifier," *IEEE Trans. Ind. Appl.*, vol. 41, no. 5, pp. 1281–1291, Sep. 2005.
- [51] S. G. Parker, B. P. McGrath, and D. G. Holmes, "Regions of active damping control for LCL filters," *IEEE Trans. Ind. Appl.*, vol. 50, no. 1, pp. 424–434, Jan. 2014.
- [52] L. Harnefors, M. Bongiorno, and S. Lundberg, "Input-admittance calculation and shaping for controlled voltage-source converters," *IEEE Trans. Ind. Electron.*, vol. 54, no. 6, pp. 3323–3334, Dec. 2007.
- [53] M. Cespedes and J. Sun, "Impedance modeling and analysis of grid-connected voltage-source converters," *IEEE Trans. Power Electron.*, vol. 29, no. 3, pp. 1254–1261, Mar. 2014.
- [54] B. Wen, D. Boroyevich, P. Mattavelli, Z. Shen, and R. Burgos, "Influence of phase-locked loop on input admittance of three-phase voltage-source converters," in *Proc. 28th Annu. IEEE Appl. Power Electron. Conf. Expo.*, Mar. 2013, pp. 1–8.

- [55] O. Goksu, R. Teodorescu, C. L. Bak, F. Iov, and P. Carne, "Instability of wind turbine converters during current injection to low voltage grid faults and PLL frequency based stability solution," *IEEE Trans. Power Syst.*, vol. 29, no. 4, pp. 1683–1691, Jul. 2014.
- [56] A. H. K. Alaboudy, H. H. Zeineldin, and J. L. Kirtley, "Microgrid stability characterization subsequent to fault-triggered islanding incidents," *IEEE Trans. Power Del.*, vol. 27, no. 2, pp. 658–669, Apr. 2012.
- [57] Z. Zou, G. Buticchi, M. Liserre, A. M. Kettner, and M. Paolone, "Voltage stability analysis using a complete model of grid-connected voltage-source converters," in *Proc. IEEE Energy Convers. Congr. Expo.*, Milwaukee, WI, USA, Sep. 2016, pp. 1–8.
- [58] A. Griffo and J. Wang, "Large signal stability analysis of aircraft power systems with constant power loads," *IEEE Trans. Aerosp. Electron. Syst.*, vol. 48, no. 1, pp. 477–489, Jan. 2012.
- [59] R. Majumder, "Some aspects of stability in microgrids," *IEEE Trans. Power Syst.*, vol. 28, no. 3, pp. 3243–3252, Aug. 2013.
- [60] J. Sun, "Small-signal methods for ac distributed power systems—A review," *IEEE Trans. Power Electron.*, vol. 24, no. 11, pp. 2545–2554, Nov. 2009.
- [61] M. Kabalan, P. Singh, and D. Niebur, "Large signal Lyapunov-based stability studies in microgrids: A review," *IEEE Trans. Smart Grid*, vol. 8, no. 5, pp. 2287–2295, Sep. 2017.
- [62] M. Kabalan, P. Singh, and D. Niebur, "A design and optimization tool for inverter-based microgrids using large-signal nonlinear analysis," *IEEE Trans. Smart Grid*, vol. 10, no. 4, pp. 4566–4576, Jul. 2019.
- [63] W. Ren, M. Steurer, and T. Baldwin, "Improve the stability and the accuracy of power hardware-in-the-loop simulation by selecting appropriate interface algorithms," *IEEE Trans. Ind. Appl.*, vol. 44, no. 4, pp. 1286–1294, Sep. 2008.
- [64] F. Andrade, J. Cusido, and L. Romeral, "Transient stability analysis of inverter interfaced distributed generators in a microgrid system," in *Proc. 14th Eur. Conf. Power Electron. Appl.*, Birmingham, U.K., Aug. 2011, pp. 1–10.
- [65] K. Acharya, S. K. Mazumder, and I. Basu, "Reaching criterion of a three-phase voltage-source inverter operating with passive and nonlinear loads and its impact on global stability," *IEEE Trans. Ind. Electron.*, vol. 55, no. 4, pp. 1795–1812, Apr. 2008.
- [66] M. Kabalan, P. Singh, and D. Niebur, "Nonlinear Lyapunov stability analysis of seven models of a DC/AC droop controlled inverter connected to an infinite bus," *IEEE Trans. Smart Grid*, vol. 10, no. 1, pp. 772–781, Jan. 2019.
- [67] J. Alipoor, Y. Miura, and T. Ise, "Power system stabilization using virtual synchronous generator with alternating moment of inertia," *IEEE Trans. Emerg. Sel. Topics Power Electron.*, vol. 3, no. 2, pp. 451–458, Jun. 2015.
- [68] F. Andrade, K. Kampouropoulos, L. Romeral, J. C. Vasquez, and J. M. Guerrero, "Study of large-signal stability of an inverter-based generator using a Lyapunov function," in *Proc. IEEE Ind. Electron. Soc.*, Oct. 2014, pp. 1840–1846.
- [69] F. A. Rengifo, L. Romeral, J. Cusidó, and J. J. Cárdenas, "New model of a converter-based generator using electrostatic synchronous machine concept," *IEEE Trans. Energy Convers.*, vol. 29, no. 2, pp. 344–353, Jun. 2014.
- [70] H. W. Dommel, "Digital computer solution of electromagnetic transients in single and multiphase networks," *IEEE Trans. Power App. Syst.*, vol. PAS-88, no. 4, pp. 388–399, Apr. 1969.
- [71] L. Qi and S. Woodruff, "Stability analysis and assessment of integrated power systems using RTDS," in *Proc. IEEE Elect. Ship Technol. Symp.*, Jul. 2005, pp. 325–332.
- [72] P. W. Sauer, B. C. Lesieutre, and M. A. Pai, "Transient algebraic circuits for power system dynamic modelling," *Int. J. Elect. Power Energy Syst.*, vol. 15, no. 5, pp. 315–321, 1993.
- [73] C. L. DeMarco and G. C. Verghese, "Bringing phasor dynamics into the power system load flow," in *Proc. North Amer. Power Symp.*, Milwaukee, WI, USA, 1993, pp. 463–471.
- [74] P. Zhang, J. R. Marti, and H. W. Dommel, "Shifted-frequency analysis for EMTP simulation of power-system dynamics," *IEEE Trans. Circuits Syst. I*, vol. 57, no. 9, pp. 2564–2574, Sep. 2010.
- [75] M. A. Elizondo, F. K. Tuffner, and K. P. Schneider, "Three-phase unbalanced transient dynamics and power flow for modeling distribution systems with synchronous machines," *IEEE Trans. Power Syst.*, vol. 31, no. 1, pp. 105–115, Jan. 2016.
- [76] M. A. Elizondo, F. K. Tuffner, and K. P. Schneider, "Simulation of inrush dynamics for unbalanced distribution systems using dynamic-phasor models," *IEEE Trans. Power Syst.*, vol. 32, no. 1, pp. 633–642, Jan. 2017.
- [77] K. P. Schneider, F. K. Tuffner, M. A. Elizondo, J. Hansen, J. C. Fuller, and D. P. Chassin, "Adaptive dynamic simulations for distribution systems using multi-state load models," *IEEE Trans. Smart Grid*, vol. 10, no. 2, pp. 2257–2266, Mar. 2019.
- [78] M. Maniopoulos, D. Lagos, P. Kotsampopoulos, and N. Hatziaargyriou, "Combined control and power hardware in-the-loop simulation for testing smart grid control algorithms," *IET Gener. Transmiss. Distrib.*, vol. 11, no. 12, pp. 3009–3018, Sep. 2017.
- [79] P. Kotsampopoulos, F. Lehfuss, G. Lauss, B. Bletterie, and N. Hatziaargyriou, "The limitations of digital simulation and the advantages of PHIL testing in studying distributed generation provision of ancillary services," *IEEE Trans. Ind. Electron.*, vol. 62, no. 9, pp. 5502–5515, Mar. 2017.
- [80] S. Leitner, M. Yazdani, A. Mehrizi-Sani, and A. Muetze, "Small-signal stability analysis of an inverter based microgrid with internal model-based controllers," *IEEE Trans. Smart Grid*, vol. 9, no. 5, pp. 5393–5402, Sep. 2018.
- [81] Y. Li and L. Fan, "Stability analysis of two parallel converters with voltage-current droop control," *IEEE Trans. Power Del.*, vol. 32, no. 6, pp. 2389–2397, Jan. 2017.
- [82] L. G. Meegahapola, D. Robinson, A. P. Agalgaonkar, S. Perera, and P. Ciufo, "Microgrids of commercial buildings: Strategies to manage mode transfer from grid connected to islanded mode," *IEEE Trans. Sustain. Energy*, vol. 5, no. 4, pp. 1337–1347, Oct. 2014.
- [83] R. Hesse, D. Turschner, and H. P. Beck, "Micro grid stabilization using the virtual synchronous machine (VISMA)," in *Proc. Int. Conf. Renewable Energies Power Quality*, Valencia, Spain, Apr. 2009, pp. 1–6.
- [84] K. Sakimoto, Y. Miura, and T. Ise, "Stabilization of a power system with a distributed generator by a virtual synchronous generator function," in *Proc. 8th Int. Conf. Power Electron.*, Valencia, Spain, May 2011, pp. 1498–1505.
- [85] P. Rodriguez, I. Candela, and A. Luna, "Control of PV generation systems using the synchronous power controller," in *Proc. IEEE Energy Convers. Congr. Expo.*, Denver, CO, USA, Sep. 2013, pp. 993–998.
- [86] J. Morren, J. Pierik, and S. W. de Haan, "Inertial response of variable speed wind turbines," *Elect. Power Syst. Res.*, vol. 76, no. 11, pp. 980–987, 2006.
- [87] B. Johnson, M. Sinha, N. Ainsworth, F. Dorfler, and S. Dhople, "Synthesizing virtual oscillators to control islanded inverters," *IEEE Trans. Power Electron.*, vol. 31, no. 8, pp. 6002–6015, Nov. 2015.
- [88] S. D'Arco and J. A. Suul, "Virtual synchronous machines- classification of implementations and analysis of equivalence to droop controllers for microgrids," in *Proc. IEEE Grenoble Conf.*, Grenoble, France, Jun. 2013, pp. 1–7.
- [89] U. Tamrakar, D. Galipeau, R. Tonkoski, and I. Tamrakar, "Improving transient stability of photovoltaic-hydro microgrids using virtual synchronous machines," in *Proc. IEEE Eindhoven PowerTech*, Jun. 2015, pp. 1–6.
- [90] U. Tamrakar, D. Shrestha, M. Maharjan, B. P. Bhattarai, T. M. Hansen, and R. Tonkoski, "Virtual inertia: Current trends and future directions," *Appl. Sci.*, vol. 7, no. 7, pp. 1–29, Jun. 2017.
- [91] *Reciprocating Internal Combustion Engine Driven Alternating Current Generating Sets- Part 5: Generating Sets*, International Organization for Standardization Std. ISO 8528-5:2005(E), 2005.
- [92] P. A. Mendoza-Araya and G. Venkataramanan, "Stability analysis of AC microgrids using incremental phasor impedance matching," *Elect. Power Compon. Syst.*, vol. 43, no. 4, pp. 473–484, Feb. 2015.